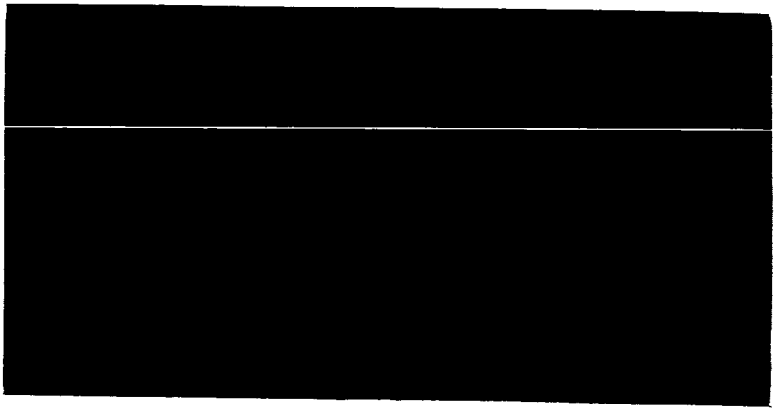

PROPAGATION OF MILLIMETER AND SUBMILLIMETER WAVES

(Final Report)

Contract NASw-963

OR 6607 July 1965

Prepared for

National Aeronautics
and Space Administration
Cambridge, Massachusetts

Prepared by: L. Frenkel
Dr. L. Frenkel

and E. P. Valkenburg
E. P. Valkenburg

Under the direction of: V. E. Derr
Dr. V. E. Derr

Approved by: A. H. Ryan
Dr. A. H. Ryan

Martin-Marietta Corporation
Orlando, Florida

FOREWORD

The work described in this report was performed under the sponsorship of National Aeronautics and Space Administration, Electronic Research Center, Cambridge, Massachusetts, under Contract NASw 963.

The work was performed at the Martin-Marietta Corporation, Orlando Division, Physical Sciences Research Laboratory, under the management of Dr. A. Ryan, during the period June 17, 1964, to June 17, 1965.

Personnel engaged in major phases of the work were:

V. E. Derr
L. Frenkel
M. Lichtenstein
E. P. Valkenburg
D. R. Wood

Credit is due to J. J. Gallagher for advice and to F. Zlotshewer for some of the calculations.

CONTENTS

Summary xi

I. A Fabry-Perot Type Resonant Cavity for Microwave Spectroscopy 1

A. Introduction 1
B. Instrumentation 5
C. Measurement Procedure 6
D. Measurement Errors 12

II. Loss Measurements in Binary Gas Mixtures Containing H_2O as One Constituent 13

A. Introduction 13
B. Experimental Method 14
C. Data Evaluation 15
D. Results 18
E. Reliability of the Data and Limitations of the Apparatus . . 22
F. Discussion 26

III. Loss Measurements on O_2 31

A. Introduction 31
B. Experimental Method and Results 31
C. Need for Additional Work 32

IV. Spectroscopic Investigation 33

A. Introduction 33
B. Search for Rotational Lines in O_2 33
C. The H_2O Molecule 34
D. NO_2 38

V. Conclusions and Recommendations 41

References 43

Appendices

A. Literature Search for Atmospheric Absorption Data 45

B. Compilation of Atmospheric Absorption Data and Extrapolation to 1000 Gc 61
C. Statement of Work 67

ILLUSTRATIONS

1	Flat Mirror Fabry-Perot Interferometer	1
2	Confocal and Semi-Confocal Fabry-Perot Interferometers	3
3	Photograph of Interferometer Removed from Vacuum	5
4	Photograph of Complete Measurement System	6
5	Block Diagram of Measurement System using Single Frequency Marker	7
6	Oscilloscope Display of Interferometer Response Showing Zero Beat Marker on Second Trace. Frequency = 183.3 Gc	8
7	Block Diagram of Measurement System using a "Fence" of Frequency Markers at 150 Gc	10
8	Oscilloscope Display of Interferometer Response Showing Zero Beat Marker "Fence" on Second Trace. Frequency = 150 Gc	11
9	Oscilloscope Display of Interferometer Response at 300 Gc. Q = 330,000	11
10	Tan δ versus p_1^2, ν = 169.794 Gc	18
11	Tan δ p_1^2, ν = 190.000 Gc	19
12	Tan δ' versus ν, p_1 = 15 mm, p_2 = 800 mm of N_2	19
13	Tan δ versus Log p' for N_2, T = 300°K	20
14	Tan δ versus Log p' for N_2, $\nu - \nu_0$ = 1.5 Gc, T = 300°K, p_1 = 15 mm	21
15	Absorption Coefficient α Due to 7.5 mm of H_2O in 750 mm of N_2 versus Frequency ν	23
16	Absorption Coefficient α for Various Gas Systems, p_1 = 15 mm, p_2 = 750 mm	28
17	Stark Effect in H_2O at 183 Gc	37
18	Stark Effect in H_2O at 380 Gc	38
19	Approximate Peaks and Windows in Atmospheric Attenuation, p = 760 mm Hg, 50 Percent Humidity (After Zhevakin and Naumov)	65

TABLES

Ia Results for Group 1 Measurements (100 to 200 Mc from the Line Center at 183.31 Gc) 21

Ib Results for Group 2 Measurements (1 to 3 Gc from the Line Center at 183.31 Gc) 21

II Linewidth Parameter in Mc/mm 22

III Comparison of Linewidth Parameters at 183.31 Gc 29

IV Rotational Transitions Predicted in O_2 34

V Predicted and Observed Transitions in H_2O Below 600 Gc . . . 35

VI Transition Tentatively Assigned to NO_2 39

VII Atmospheric Absorption, Oxygen 62

VIII Water Vapor Attenuation 63

IX Total Atmospheric Absorption (db/km) 64

SUMMARY

The communications problems in space flight differ from those on the earth's surface in various ways, including the propagation properties of the atmospheres encountered on a particular mission. Space flight communication may be able to utilize frequency regions of the spectrum to which the earth atmosphere is opaque and, perhaps, will exclude the use of some frequencies which are useful in terrestrial communications.

A knowledge of submillimeter wave propagation through atmospheres must be based upon three separate disciplines. These are 1) the study of the composition and physical state of the atmosphere, 2) the spectroscopy of the molecular species involved and 3) the study of the effects of intermolecular interactions upon the nonresonant dielectric behavior of compressed gases.

This report describes in several more or less self-contained chapters work in the last two of these areas. According to the work statement (Appendix C), the work included studies of the resonant peaks as well as the off-resonant regions of the absorption spectra of atmospheric gases at frequencies up to 300 Gc and the efforts will be extended under the terms of a follow-on contract toward higher frequencies.

The study of the nonresonant dielectric behavior in the laboratory requires sensitive absorption cells, and Chapter I of this report describes the development of a compact, practical and precise instrument equivalent to an absorption cell several hundred feet long. The instrument is based upon the principles of Fabry-Perot interferometry; it has a sensitivity of $\tan \delta \approx 10^{-8}$ and may be used for spectroscopy as well as for absorption measurements.

Chapter II deals with absorption measurement in H_2O and its mixtures in the frequency region between 150 and 300 Gc. Section C of that chapter deals with a method for evaluating the linewidth parameters which has not hitherto been applied to problems of this nature. The results, reported in Section D of that chapter, bring out a number of new features, notably a very large effect upon the wing absorption by pure H_2O and CO_2.

Chapter III gives some preliminary results for oxygen which indicate that H_2O - O_2 mixtures do not behave in an anomalous manner.

Chapter IV reports work on the low pressure spectroscopy of O_2, H_2O, and NO_2. In H_2O several lines were observed for the first time and the transition frequencies located precisely. Stark measurements on some of these are reported. The search for rotational lines in O_2 has not been successful so far, and some difficulties encountered in the search are described in Section A. Several groups of lines have been found in NO_2; efforts to assign these are now in progress.

The work reported here has concentrated on providing fundamental data of general usefulness. The comments and recommendations in Chapter V emphasize this aspect and point out problems in this area, which are of interest in connection with planetary atmospheres.

Appendix A is a critical survey of existing data on atmospheric absorption. This appendix and its references and the figures in it are completely self-contained.

Compilations of data on atmospheric absorption as a function of altitude are included in the references cited in Appendix A. The measurements of this report are in close agreement with the values calculated by Schmelzer. For convenience, these data are quoted in Appendix B.

I. A FABRY-PEROT TYPE RESONANT CAVITY FOR MICROWAVE SPECTROSCOPY

A. INTRODUCTION

The use of resonant structures to observe molecular resonances and measure the associated absorption coefficients is not of recent origin (References 1, 2, and 3). In the millimeter wavelength region, however, the cylindrical waveguide cavities normally employed at lower frequencies are limited in Q by wall losses and mechanical tolerances. This problem has been greatly alleviated by the microwave equivalent of the Fabry-Perot (F-P) interferometer (References 4 through 8).

The F-P interferometer has recently found application in laser technology (References 9, 10 and 11). A brief review of operating principles, and results of extensive analyses, is appropriate at this point.

The basic interferometer shown in Figure 1 consists of two partially reflecting flat mirrors separated by many wavelengths. When illuminated by a monochromatic plane wave, resonances occur at half wavelength intervals in mirror separation.

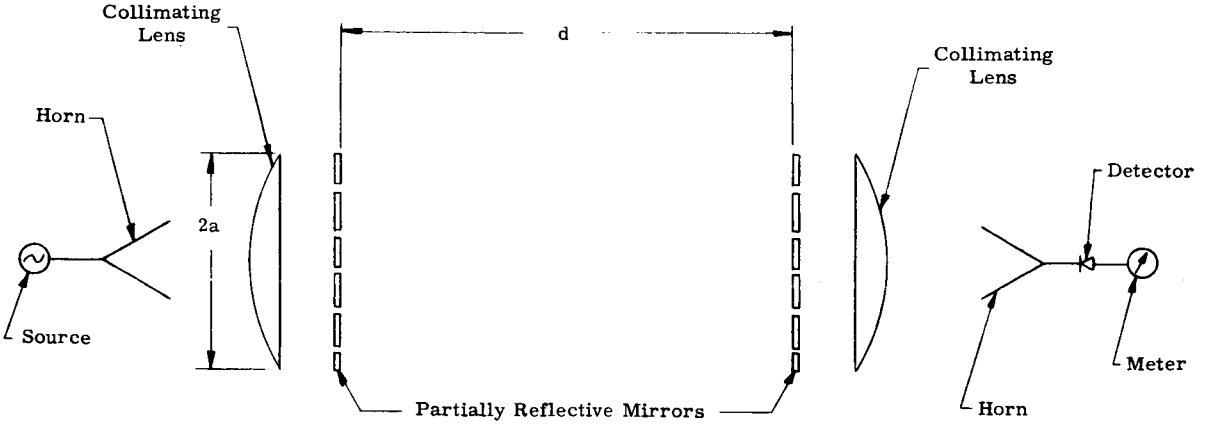

Figure 1. Flat Mirror Fabry-Perot Interferometer

The Q of the interferometer for a given plate separation is limited by mirror loss and diffraction loss beyond the mirror edges. Mirror loss is a function of the resistivity of the material employed and the transmission coefficient of the mirrors, each of which can be controlled without difficulty. Diffraction loss can be minimized by a proper choice of mirror size for a given mirror separation. However, slight misalignment of the mirrors from parallelism will drastically increase diffraction losses and destroy the high Q obtainable with large plate separations.

To ease the mirror alignment problem a pair of spherical confocal mirrors may be employed as shown in Figure 2. The resonant modes that the resulting confocal resonator can support are commonly designated by the notation TEM_{qmn}

where

q = number of intergral half wavelengths between mirrors;

m = number of field reversals in a direction transverse to the interferometer axis of symmetry;

n = number of field reversals in a transverse direction which is orthogonal to the direction assumed for m.

The integer q is very large($\approx 10^3$) for high Q resonators and is usually omitted, resulting in a mode notation of TEM_{mn}.

The conditions of resonance for a spherical mirror resonator are given by

$$\frac{4d}{\lambda} = 2q + (1+m+n)\left[1 - \frac{4}{\pi}\tan^{-1}\frac{b-d}{b+d}\right] \qquad (1)$$

where

d = mirror separation

b = mirror radius

λ = wavelength at resonance

m,n,q = as defined above.

When the mirrors are separated by their equal radii of curvature, b = d and the system is confocal. Under these conditions resonance occurs when

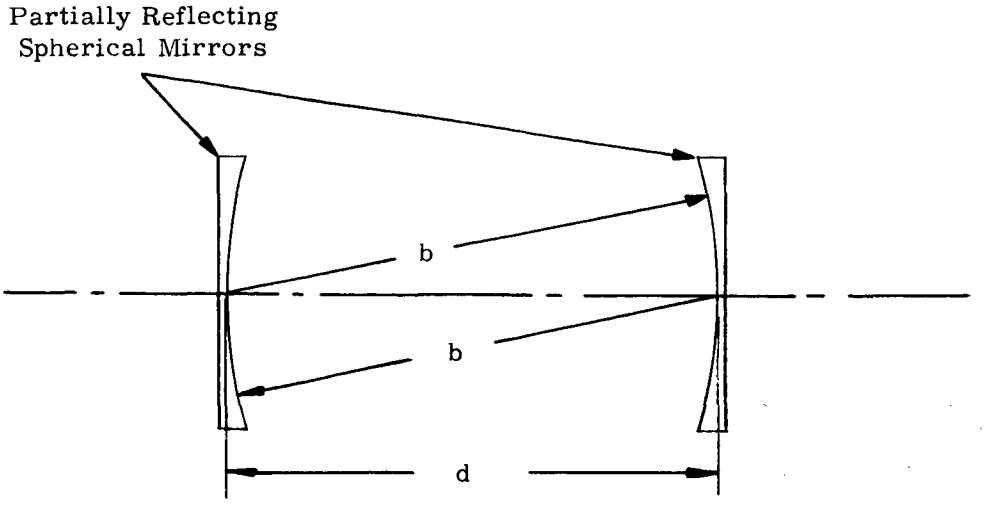

Confocal Interferometer
Mirror Radius (b) Equals Mirror Separation (d)

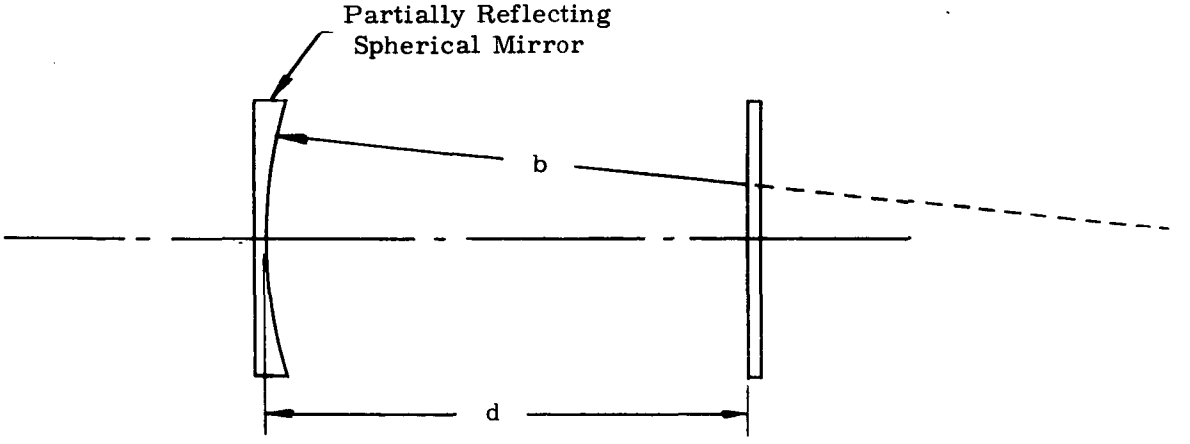

Semiconfocal Interferometer
Radius of Curved Mirror (b) Equals
Twice Mirror Separation (2d)

Figure 2. Confocal and Semi-Confocal Fabry-Perot Interferometers

$$\frac{4b}{\lambda} = 2q + (1+m+n). \qquad (2)$$

Note that the quantity $4b/\lambda$ of equation (2) must take on integral values. This requirement is not imposed on $4d/\lambda$ of equation (1) as a condition for

resonance of a nonconfocal system. Also, the modes associated with the confocal system are degenerate in (m+n). This degeneracy is removed in the nonconfocal case. For the dominant mode, m=n=0 and equations (1) and (2) simplify accordingly.

The Q of the F-P resonator in terms of the mirror spacing, d, is given by

$$Q = \frac{2\pi}{\alpha\lambda} d \tag{3}$$

where α is resonator power loss consisting of reflection loss, diffraction loss and loss in the propagation medium between the reflectors. Since these losses are additive, Equation (3) can be used to determine the loss of the medium by measuring the Q in vacuum, Q_1, and the Q with a gas as a propagation medium, Q_2, at known temperatures and pressures. Under these conditions the power loss factor, α, of the gas introduced can be obtained from the expression:

$$\alpha = \frac{2\pi}{\lambda} \left(\frac{1}{Q_2} - \frac{1}{Q_1}\right) \text{cm}^{-1} \tag{4}$$

If "A" is the output of a square law detector loosely coupled to the output of the F-P resonator, then $Q_1/Q_2 = (A_1/A_2)^{\frac{1}{2}}$ and equation (4) becomes

$$\alpha = \frac{2\pi}{\lambda Q_1} \left[(A_1/A_2)^{\frac{1}{2}} - 1\right] \text{cm}^{-1} \tag{5}$$

When expressed in terms of db per kilometer, Equation (5) becomes:

$$\alpha = \frac{27.27 \times 10^6}{\lambda Q_1} \left[(A_1/A_2)^{\frac{1}{2}} - 1\right] \text{db/km} \tag{6}$$

where λ is expressed in millimeters.

Equation (5) implies that the effective path length of the F-P resonator is given by

$$\text{EPL} = \frac{Q_1 \lambda}{2\pi} . \tag{7}$$

The advantage of a high Q is apparent from Equations (5) through (7) when a measurement of very low losses is required. For a frequency of 300 Gc ($\lambda = 3.34 \times 10^{-3}$ feet) and a Q of 10^6, the effective absorption path length is 530 feet.

According to equation (3) this can be done with a semi-confocal interferometer less than 2 feet in length, as opposed to a propagation waveguide cell 530 feet in length.

B. INSTRUMENTATION

The semiconfocal interferometer shown in Figure 3 was designed for an approximate unloaded Q of 10^6. The mirror diameters were not chosen to meet the conditions set forth by Fox and Li[9] for the suppression of higher order modes, i.e., $\alpha^2/b\lambda \approx 1$ where 2α = mirror diameter and b = mirror radius of curvature. Instead, in order to accommodate frequency changes more easily, a constricting iris of Viton vacuum seal rubber was used to provide a circular opening slightly larger than the beam size at the midpoint between the reflectors. In addition, a bakelite dielectric tube of 6 inches diameter and 3/16 inch wall thickness was mounted coaxially in the iris. The combination of lossy iris and dielectric tube served to suppress modes higher than the fundamental TEM_{oo} mode and minimize reflections from the vacuum chamber walls.

The semiconfocal mirror separation is 24 inches and the mirror diameters are 9 inches. The radius of curvature of the curved mirror is 48

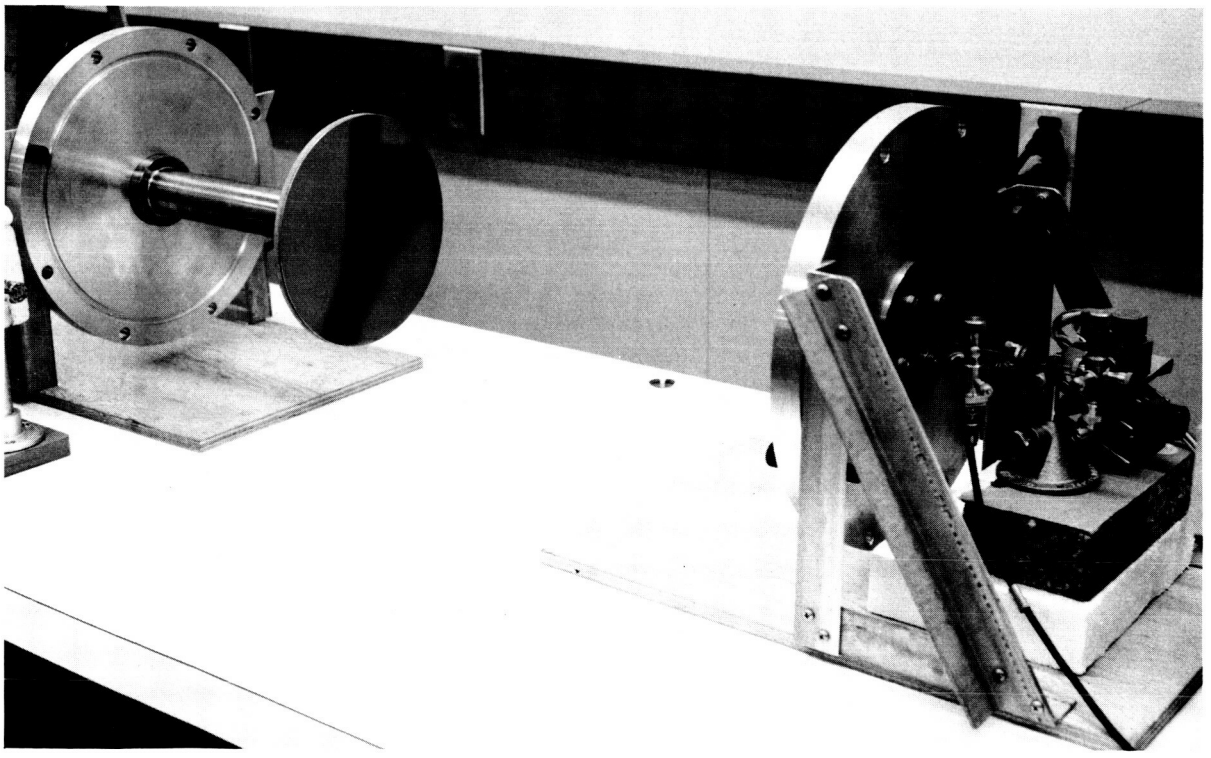

Figure 3. Photograph of Interferometer Removed from Vacuum

inches. Mirrors were optically ground from stainless steel blanks to a surface tolerance of a few microns, gold plated, and polished. The curved mirror is mounted on a threaded steel shaft (80 threads per inch) to facilitate tuning the interferometer.

Input and output RG-135/U waveguides were coupled into the interferometer as close to the center of the flat mirror as possible. These waveguides were initially terminated in circular irises in an attempt to couple as loosely as possible to the interferometer. However, it was found that, because of the low RF power sources available, the waveguide irises had to be removed in order to obtain sufficient signal-to-noise ratio at the detector.

A photograph and typical block diagram of the measurement system are shown in Figures 4 and 5. Instruments are referenced by number and listed in Table I.

C. MEASUREMENT PROCEDURE

The basic measurement procedure is directed toward the use of Equation (6) to determine the loss, α, of water vapor as a function of water vapor density and pressure, using nitrogen, oxygen and carbon dioxide as the foreign gases.

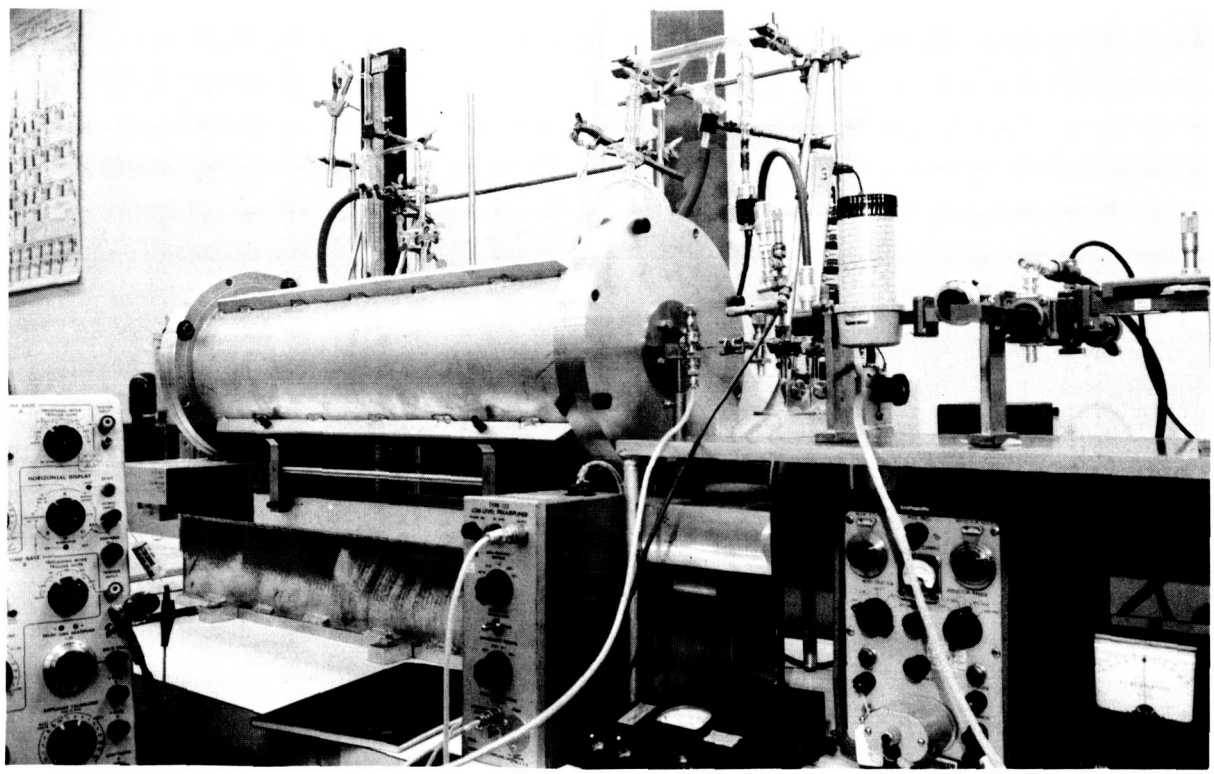

Figure 4. Photograph of Complete Measurement System

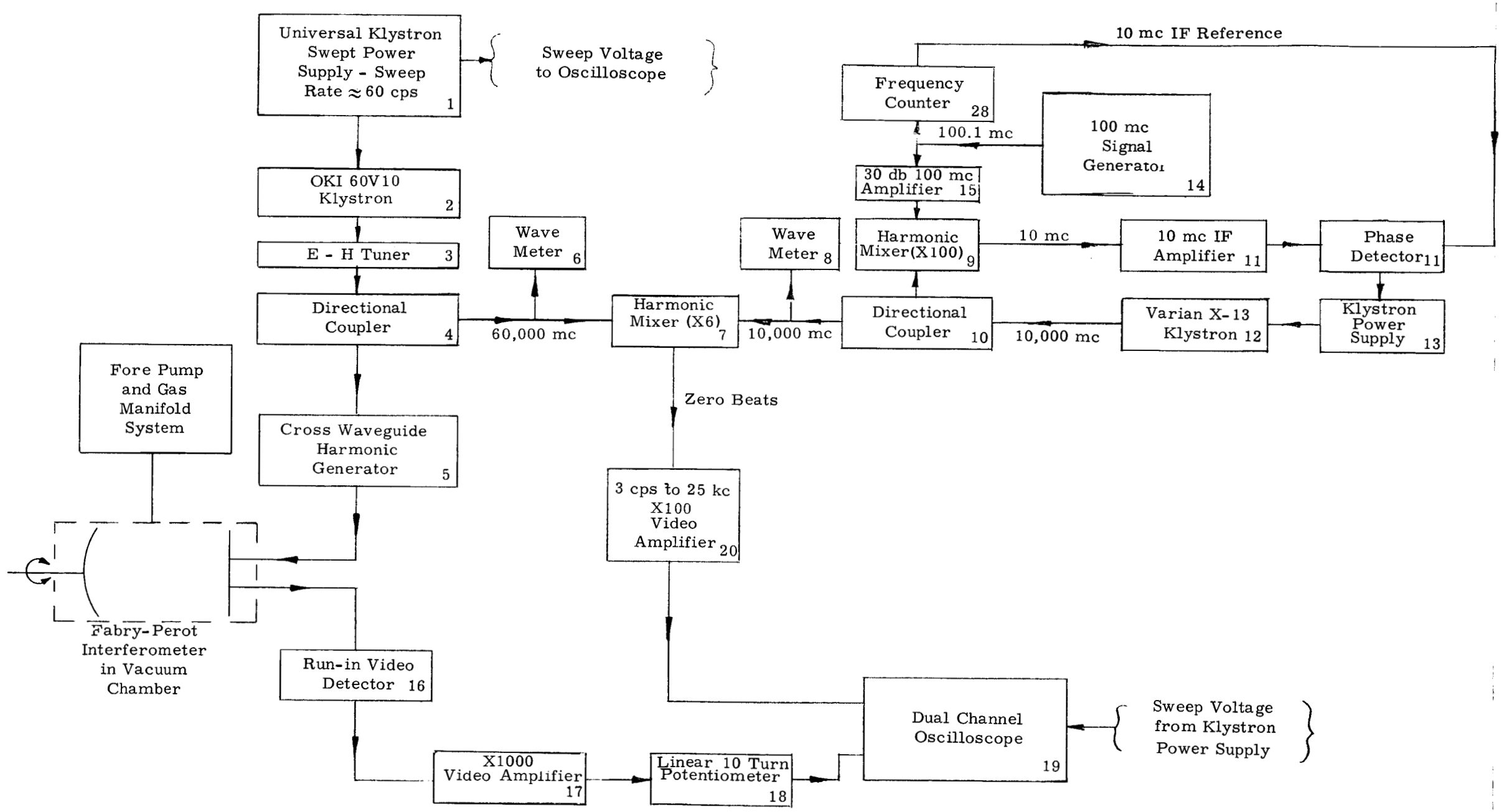

1. PRD Type 812 Klystron Power Supply
2. OKI 60V10 Klystron 55-65 Gc ≈ 100 mw
3. FXR Model M312C RG-98 E-H Tuner
4. FXR Model MA774C RG-98 Directional Coupler
5. RG-98/RG-135 Run-in Multiplier Constructed by Rogers
6. FXR Model M410X RG-98 Wavemeter
7. FXR Model M206B RG-98 Detector
8. Hewlett-Packard X532B X-Band Wavemeter
9. Somerset Radiation Laboratory Model X802 Diode Multiplier and Hewlett-Packard Model X485B X-Band Detector Mount
10. Hewlett-Packard Model X750D 20 db X-Band Cross-Guide Coupler
11. Martin Constructed Phase-Lock System
12. Varian X-13 X-Band Klystron Tube
13. Hewlett-Packard Model 715A Power Supply
14. Hewlett-Packard Model 608C Signal Generator
15. Martin Constructed 100 mc 30 db Gain Amplifier
16. Rogers Constructed RG-135 Run-in Detector
17. Tektronix Type 122 Low-Level Pre-Amplifier X1000 Gain
18. IRC Ten-Turn 10K 0.1 Percent Linear Potentiometer
19. Tektronix Type 535A Oscilloscope with Dual-Trace Pre-Amplifier
20. Tektronix Type 123 Video Pre-Amplifier
21. Varian VA-714E Klystron 142-150 Gc ≈ 135 mw
22. TRG Model G620 RG-135 E-H Tuner
23. TRG Model G-561 10 db RG-135 Directional Coupler
24. TRG Model G-550 RG-135 Wavemeter
25. GR Type 1211B Unit Oscillator 0.5-50 mc
26. UG-119A Video Detector
27. LEL Model IF 30DP 30 mc IF Amplifier with Video Detector
28. Hewlett-Packard 524B Electronic Counter

Figure 5. Block Diagram of Measurement System Using Single Frequency Marker

The vacuum chamber is first evacuated with the fore pump to a pressure of about 25 to 30 microns. The evacuated Q of the interferometer (Q_1 of Equations 5 and 6) is then measured. This is accomplished by displaying frequency markers (zero beats) on the face of an oscilloscope along with the detected output of the interferometer.

As the millimeter wave klystron (60V10) is linearly swept with a sawtooth reflector modulation voltage, the frequency response of the interferometer is displayed on the oscilloscope. As shown in Figure 5, the swept frequency output of the primary RF source (60V10 klystron) is sampled by a directional coupler prior to multiplication from 60 Gc to 180 Gc in the crossed guide harmonic generator feeding the interferometer. A zero beat is then produced between the sampled 60 Gc swept signal and the sixth harmonic of a phase locked Varian X-13 klystron as shown in Figure 5.

By adjusting the frequency of the 100 mc signal generator in the phase-lock loop of Figure 5, the frequency of the X-13 klystron can be adjusted to place the zero beat at the maximum and the half power points of the displayed interferometer response curve. The frequency of the 100 Mc signal generator is measured with a frequency counter as shown, permitting the determination of the OKI 60V10 frequency to an accuracy of one part in 10^8. These data were used to determine Q_1 and λ of Equation (6). A photograph of the interferometer response showing the zero beat marker is shown in Figure 6.

Once Q_1 and λ have been determined with the above procedure, water vapor is introduced into the vacuum chamber containing the interferometer by opening the water flask valve on the manifold until the desired partial pressure

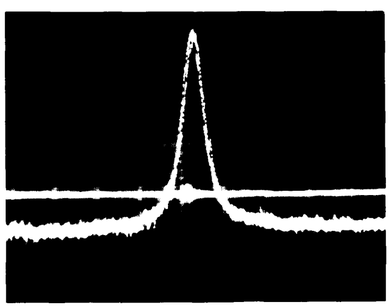

Figure 6. Oscilloscope Display of Interferometer Response Showing Zero Beat Marker on Second Trace. Frequency = 183.3 Gc

(density) is obtained. By so doing, the dielectric constant of the medium between the interferometer mirrors will change and the interferometer tuning must be slightly adjusted by changing the mirror separation to maintain a resonant condition. As a result of water vapor loss, the detected output of the interferometer will be reduced from A_1, corresponding to an evacuated condition, to A_2, corresponding to the reduced system Q. The amount of this reduction is determined by removing enough video attenuation with the linear helipot to bring the output response back to its original level. The ratio of helipot settings then corresponds to the required ratio A_1/A_2 of Equation (6), and the loss, α, can be calculated.

In addition to water vapor loss versus altitude (pressure) for various densities, these data may be used to determine self-broadening and foreign gas broadening parameters for water vapor as described elsewhere in this report.

It should be noted that retuning of the interferometer is required each time the pressure is changed. The tuning adjustments result in a total change in mirror separation of about 0.025 inch. Because of the large initial mirror separation (24 inches) this retuning will produce a Q change less than 0.1 percent. This error can be ignored compared to the error in Q measurement discussed in the following section.

The use of a Varian VA-714E klystron operating at 150 Gc eliminated the need for a cross guide harmonic generator and resulted in more power at the interferometer input waveguide terminals. However, frequency marker (zero beat) generation was not possible using the technique described above. This was due to the large multiplication (x 15) required of the X-band phase locked frequency.

As a result, the marker generator system shown in Figure 7 was employed as a unique method for producing a series or "fence" of zero beats of accurately known separation. These zero beats are obtained by mixing the harmonics of a stable unit oscillator (Nxf_m) with the swept 30 mc IF signal derived from the VA-714E klystron and the phase locked X-13. The swept 30 Mc IF signal is obtained by harmonic mixing the sampled output of the VA-714E klystron with the fifteenth harmonic of the phase locked Varian X-13 klystron. By adjusting the unit oscillator frequency, f_m, a zero beat can be placed at each of the half power points of the displayed resonance response of the interferometer. The width of the response curve is then given directly by the unit oscillator frequency as measured with a frequency counter.

The frequency of interferometer resonance is obtained by adjusting the unit oscillator to 30 Mc (or some known sub-multiple thereof) and adjusting

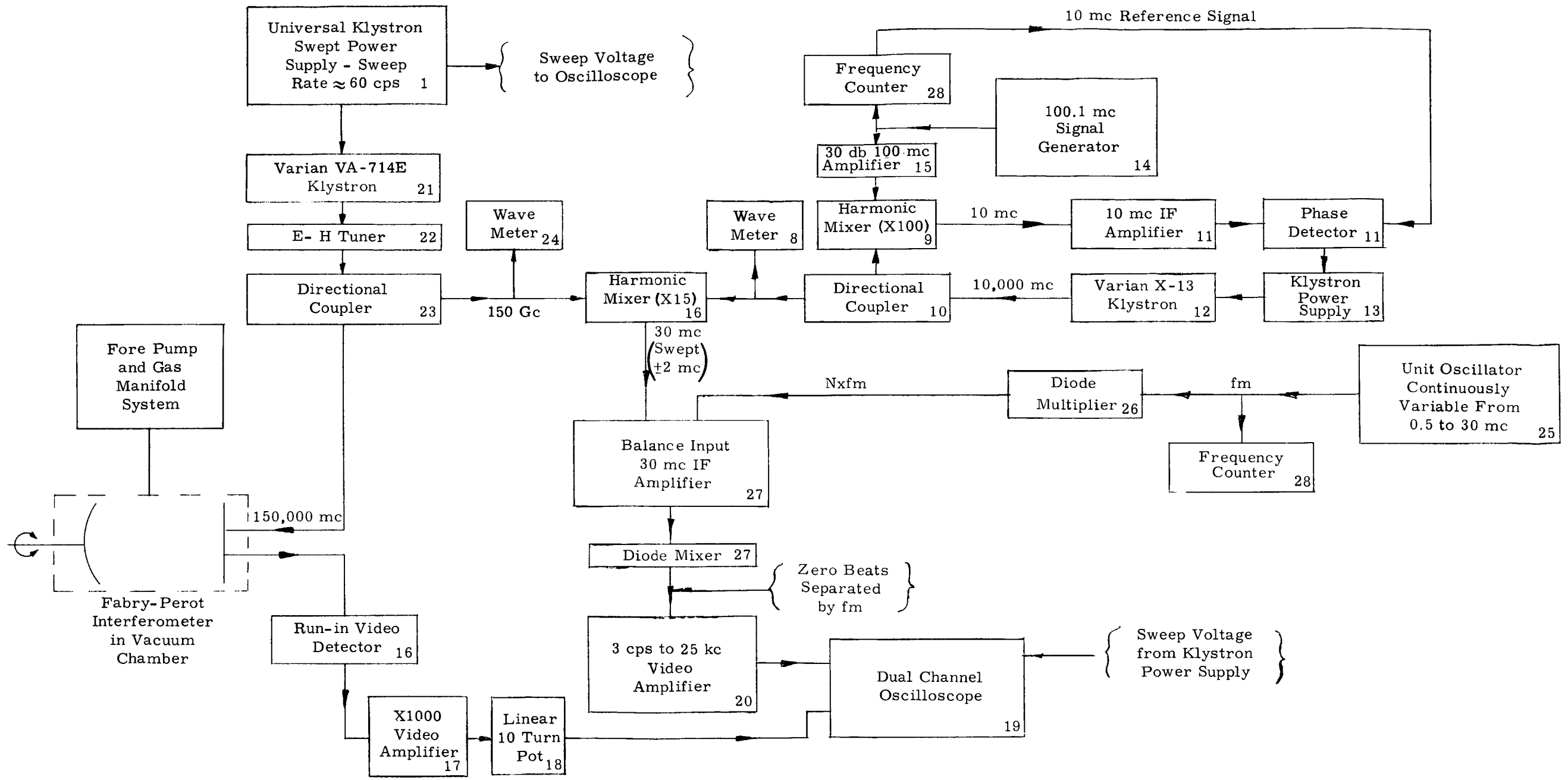

1. PRD Type 812 Klystron Power Supply
2. OKI 60V10 Klystron 55-65 Gc ≈ 100 mw
3. FXR Model M312C RG-98 E-H Tuner
4. FXR Model MA774C RG-98 Directional Coupler
5. RG-98/RG-135 Run-in Multiplier Constructed by Rogers
6. FXR Model M410X RG-98 Wavemeter
7. FXR Model M206B RG-98 Detector
8. Hewlett-Packard X532B X-Band Wavemeter
9. Somerset Radiation Laboratory Model X802 Diode Multiplier and Hewlett-Packard Model X485B X-Band Detector Mount
10. Hewlett-Packard Model X750D 20 db X-Band Cross-Guide Coupler
11. Martin Constructed Phase-Lock System
12. Varian X-13 X-Band Klystron Tube
13. Hewlett-Packard Model 715A Power Supply
14. Hewlett-Packard Model 608C Signal Generator
15. Martin Constructed 100 mc 30 db Gain Amplifier
16. Rogers Constructed RG-135 Run-in Detector
17. Tektronix Type 122 Low-Level Pre-Amplifier X1000 Gain
18. IRC Ten-Turn 10K 0.1 Percent Linear Potentiometer
19. Tektronix Type 535A Oscilloscope with Dual-Trace Pre-Amplifier
20. Tektronix Type 123 Video Pre-Amplifier
21. Varian VA-714E Klystron 142-150 Gc ≈ 135 mw
22. TRG Model G620 RG-135 E-H Tuner
23. TRG Model G-561 10 db RG-135 Directional Coupler
24. TRG Model G-550 RG-135 Wavemeter
25. GR Type 1211B Unit Oscillator 0.5-50 mc
26. UG-119A Video Detector
27. LEL Model IF 30DP 30 mc IF Amplifier with Video Detector
28. Hewlett-Packard 524B Electronic Counter

Figure 7. Block Diagram of Measurement System Using a "Fence" of Frequency Markers at 150 Gc

the X-13 frequency (obtained from the frequency counter) until a zero beat is superimposed on the peak of the response curve. With the aid of the wavemeters to obtain multiplication factors, the frequency of the VA-714E can be determined to one part in 10^8 at the peak of the interferometer response curve. A photograph of the oscilloscope trace of the interferometer response at 150 Gc and the zero beat markers is shown in Figure 8. The interferometer response at 300 Gc (second harmonic of VA-714E) is shown in Figure 9.

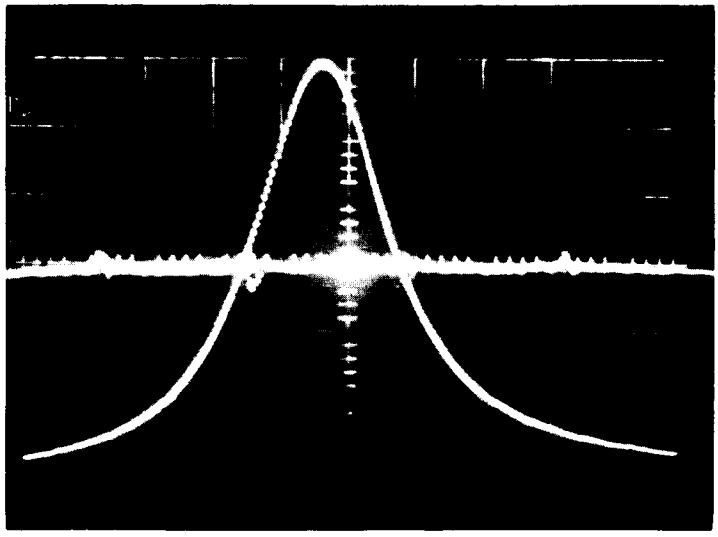

Figure 8. Oscilloscope Display of Interferometer Response Showing Zero Beat Marker "Fence" on Second Trace. Frequency = 150 Gc

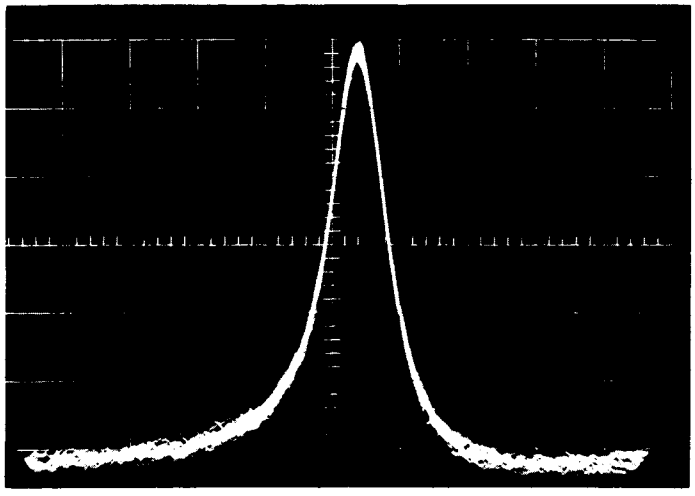

Figure 9. Oscilloscope Display of Interferometer Response at 300 Gc. Q = 330,000

D. MEASUREMENT ERRORS

Repetitive measurements have shown that, for a given loss, the position of the oscilloscope trace can be repetitively reset to a given position on the face of the oscilloscope to within 0.5 percent of the helipot digital readout. This error in amplitude is equivalent to an error in amplitude ratio $A_1/A_2 = 1.005$. The error in the loss corresponding to this ratio error can be obtained from Equation (7) as,

$$\Delta\alpha = \pm \frac{6.82 \times 10^4}{\lambda Q_1} \tag{8}$$

At 183 Gc, $\lambda = 1.64$ mm and when $Q_1 = 3 \times 10^5$, $\Delta\alpha = 0.14$ db/kilometer. At 300 Gc, the corresponding error is 0.23 db/kilometer.

Since frequency is measured to an accuracy of one part in 10^8, the contribution of wavelength to measurement errors is negligible. The contribution of errors in the measurement of Q_1, however, is significant, and will predominate over amplitude and wavelength errors. As a result of repetitive measurements, it is estimated that the error in measuring Q by the method described in section C is approximately 5 percent, resulting in an equivalent error in loss, α. The total maximum error of measurement from all sources, therefore, will be approximately

$$E_\alpha = \pm (\Delta\alpha + 1.05\ \alpha) \text{ db/kilometer} \tag{9}$$

II. LOSS MEASUREMENTS IN BINARY GAS MIXTURES CONTAINING H_2O AS ONE CONSTITUENT

A. INTRODUCTION

The microwave absorption of water vapor and its mixtures with other gases has received a great deal of experimental and theoretical attention over the past 20 years. Measurements have been interpreted on the basis of the equations of Van Vleck and Weisskopf (1945) (Reference 12) and Van Vleck (1947) (Reference 13). Various values of the linewidth parameter $\Delta\nu/p$ have been quoted to bring measured values of the absorption into agreement with theory, and it has been suggested that the wing absorption may be characterized by a different parameter than the line centers.

The data of Becker and Autler (1946), (Reference 14) for example, can be interpreted by assuming a $\Delta\nu/p$ of 4 Mc/mm Hg for H_2O - N_2 collisions in the center of the lines and a parameter of about 18 Mc/mm Hg in the wings. More recently Rusk (1965) (Reference 15) has shown that low pressure measurements at the line center are consistent with linewidth parameters of 4 Mc/mm and 20 Mc/mm for H_2O - N_2 and H_2O - H_2O collisions respectively. Earlier data by Tolbert and his collaborators (1958-1963) (References 16, 17, and 18) had produced parameters varying between 7 and 11 Mc/mm for H_2O - N_2 collisions and the suggestion that some anomalies might be caused by undiscovered lines near 120 Gc.

One difficulty in reconciling these data lies in the variety of experimental conditions under which the measurements were made and it has, therefore, not been possible to obtain a single expression which would permit the calculation of the microwave attenuation through mixtures of gases containing water vapor.

In the present research the microwave attenuation at frequencies between 120 and 300 Gc was measured for various pure gases and synthetic gas mixtures in a Fabry-Perot resonant cavity capable of detecting loss tangents of $\tan\delta \approx 0.1 \times 10^{-7}$. This sensitivity allowed the determination of losses in pure H_2O vapor and its mixtures some distance into the wings of the lines and it became possible to sort out the various contributions to the linewidth parameters so that a reasonably versatile formula for the absorption could be established. It turns out that the collision parameters in the

center of the lines at high pressures are close to those measured by Rusk at low pressures and predicted theoretically by Benedict and Kaplan (1959) (References 19 and 20). The background absorption is substantially higher than calculated by Van Vleck and can be approximately represented by a term four times the theoretical value in H_2O - N_2 collisions. This term does, however, also contain contributions from H_2O - H_2O collisions which are very much more efficient in causing absorption in the background. A linewidth parameter as high as 200 Mc/mm must be assumed. Of course the equations of Van Vleck and Weisskopf are not valid over all of this region since the linewidth parameters can clearly not be regarded as constant. For this reason it is convenient, though probably no more correct, to represent the absorption lines by individual Lorentz terms and the regions in between by terms proportional to powers of various parameters such as frequency and pressure. The purpose of the present research then may be restated to be the determination of the coefficients of the various terms.

B. EXPERIMENTAL METHOD

The principles of measuring loss tangents in resonant, transmission type cavities are well established (J. C. Slater (1946) (Reference 21). Three basic types of measurements are possible:

1 Measurements of optical pathlength

2 Measurements of transmitted power

3 Measurements of response shape (Q).

The extraction of absorption data from the dispersion measurements is rather difficult and for this reason only the power and shape measurements were used in this work. As pointed out by G. Birnbaum (1954) (Reference 22) these two measurements are independent so far as various instrumental difficulties are concerned and a simultaneous measurement of the transmission changes and the Q changes on admitting a gas, therefore, provides a sensitive check on the linearity of the apparatus. On the other hand, change in amplitude can be measured with much greater sensitivity than Q changes so that this crosscheck is available only near the absorption lines where the losses are large.

By employing various refinements it is possible to read the amplitudes to 0.3 percent (L. Frenkel, 1964) (Reference 23). Details of the performance of the instrument are given under "Reliability and Accuracy," below.

C. DATA EVALUATION

To discuss various experimental procedures which were employed it is necessary to start with an assumed equation for the absorption. The following expressions for the loss tangent and the absorption coefficients, respectively, serve this purpose:

$$\frac{\tan\delta}{p_1} = C_{01}^{t} \frac{\nu\, k_{12}^{o}\, p_0'}{(\nu-\nu_{01})^2 + (k_{12} p_0')^2} + C_{02}^{t} \frac{\nu\, k_{12}^{o}\, p_0'}{(\nu-\nu_{02})^2 + (k_{12}^{o}\, p_0')^2}$$

$$+ C_{w}^{t} \frac{\nu\, k_{12}^{w}\, p_w'}{\nu_{0w}^2} \qquad (10)$$

and

$$\frac{\alpha}{p_1} = C_{01}^{\alpha}\left(\frac{\nu}{\nu_{01}}\right) \frac{\nu\, k_{12}^{o}\, p_0'}{(\nu-\nu_{01})^2 + (k_{12}^{o}\, p_0')^2} + C_{02}^{\alpha}\left(\frac{\nu}{\nu_{02}}\right) \frac{\nu\, k_{12}^{o}\, p_0'}{(\nu-\nu_{02})^2 + (k_{12}^{o}\, p_0')^2}$$

$$+ C_{w}^{\alpha} \frac{\nu^2\, k_{12}^{w}\, p_w'}{\nu_{0w}^3} \qquad (11)$$

The first two terms represent the two absorption lines in the region of interest, i.e., at $\nu_{01} = 183.31$ and $\nu_{02} = 325$ Gc. The last term takes care of the background in first approximation. The primed pressures are "effective" pressures to be compiled as below:

$$p_0' = (k_{11}^{o}\, p_1 + k_{12}^{o}\, p_2)/k_{12}^{o} \qquad (12a)$$

and

$$p_w' = (k_{11}^{w}\, p_1 + k_{12}^{w}\, p_2)/k_{12}^{w} \qquad (12b)$$

where p_1 is the partial pressure of H_2O and p_2 that of the foreign gas. The constants C_0 may be calculated using theoretical linestrengths (King, Hainer and Cross, 1947) (Reference 24). The constants C_w may be adjusted so as to agree with the corresponding values given for the background by Van Vleck. At a temperature of 300°K

$$C_{01}^{t} = 3.53 \times 10^{-9} \quad C_{02}^{t} = 1.26 \times 10^{-9} \quad C_{w}^{t} = 1.52 \times 10^{-7}$$

$$C_{01}^{\alpha} = 0.0586 \quad C_{02}^{\alpha} = 0.0374 \quad C_{w}^{\alpha} = 2.55 \text{ (db/km)}$$

α is then given in db/km. The frequency ν_{0w} has been chosen as 183.31 Gc.

To determine the constants k in Equation (12) one can select regions of frequency and pressure where only one or two of the constants are important. In the wing region, for example, only the last term is important.

For pure H_2O Equation (12b) becomes

$$p_w' = p_1 \frac{k_{11}^{w}}{k_{12}^{w}} \tag{13}$$

so that from (12a)

$$\tan\delta = p_1^{2} C_w^{t} \frac{\nu}{\nu_{0w}^{2}} k_{11}^{w} \tag{14}$$

since C_w^{b}, ν and ν_{0w} are known k_{11}^{w} can be determined from a straight line plot of $\tan\delta$ against $(p_1)^2$.

To determine k_{12}^{w}, one has, at high partial pressures of the foreign gas:

$$p_w' \approx p_2 \tag{15}$$

so that

$$\tan\delta' = \tan\delta - C_0^{t} \frac{p_1 \nu k_{12}^{o} p_2}{(\nu-\nu_0)^2 - (k_{12} p_2)^2} = p_1 p_2 C_w^{t} \frac{\nu}{\nu_{0w}^{2}} k_{12}^{w} \tag{16}$$

In this case $\tan\delta'$ depends linearly on p_1 and p_2 but the ratio of p_2/p_1 must be kept large to make the approximation Equation (15) valid.

Near the line at 183.31 Gc the first term in Equation (10) predominates and for pure H_2O then

$$\tan\delta = p_1^2 C_{01}^t \frac{\nu k_{11}^o}{(\nu-\nu_0)^2 + (k_{11}^o p_1)^2} \tag{17}$$

because of the p_1 dependent term in the denominator it is in general inconvenient to work with Equation (17). Two avenues are open. One is to rearrange Equation (17) as

$$\frac{p_1^2 \nu}{\tan\delta} = (\nu - \nu_o)^2 \left(C_{01}^t \nu k_{11}^o\right)^{-1} + k_{11}^o p_1^2 \left(C_{01} \nu\right)^{-1} \tag{17a}$$

leading to a linear relation between $(\tan\delta)^{-1}$ and p_1^{-2}. The other consists of increasing $(\nu - \nu_0)$ in Equation (17) until its square is an order larger than the largest expected value of $(k_{11}^o p_1)^2$.

Since $\tan\delta$ becomes quite large in the first approach and since power is generally limited, the second approach is preferable. In this case, however, the background term is no longer negligible and must be taken into account. This leads to

$$\tan\delta \approx p_1^2 \left[C_{01}^t \frac{\nu}{(\nu-\nu_0)^2} k_{11}^o + \left(C_w^t \frac{\nu}{\nu_{w0}^2}\right) k_{11}^w\right] \tag{17b}$$

Plots of tan~ versus p_1^2 permit evaluation of k_{11}^o provided that k_{11}^w has been determined previously (Equation 14).

With k_{11}^w, k_{12}^w, and k_{11}^o determined, it becomes possible to measure k_{12}^o and the line strength independently as follows: Near the line at 183.31 the loss tangent for a fixed p_1 and ν becomes

$$\tan\delta = p_1 C_{01}^t \frac{\nu p_o' k_{12}^o}{(\nu-\nu_0)^2 + (k_{12} p_0')^2} \tag{18}$$

and is seen to be a symmetrical function of log p_0' with a maximum given by

$$\tan\delta_{max} = p_1 C_0^t \frac{\nu}{2(\nu-\nu_0)} \tag{18a}$$

when

$$k^{o}_{12}\, p'_{0\ max} = \nu - \nu_0 \qquad (19)$$

Equation (18a) depends only on well known frequencies and the partial pressure p_1 of H_2O which remains constant as the foreign gas is added so that C^t_0 can be compared to theory independently of k^o_{12}. Equation (19), on the other hand, depends only on the frequencies ν and ν_0 and the pressure $p'_{0\ max}$ at which the maximum loss occurs. As Equation (19) shows, $p'_{0\ max}$ becomes quite small as ν approaches ν_0 so that it is sometimes preferable to compromise by working a little further in the wings and adding a correction term for the background.

D. RESULTS

Figures 10 and 11 show some data taken for the determination of k^w_{11} and k^o_{11}, respectively. Using Equation (17b) at various frequencies, k^o_{11} was found to be 22 Mc/mm and k^w_{11} about 200 Mc/mm. Other data taken supported this large value but the precision of the measurement of k^w_{11} is subject to a number of systematic errors which are hard to detect.

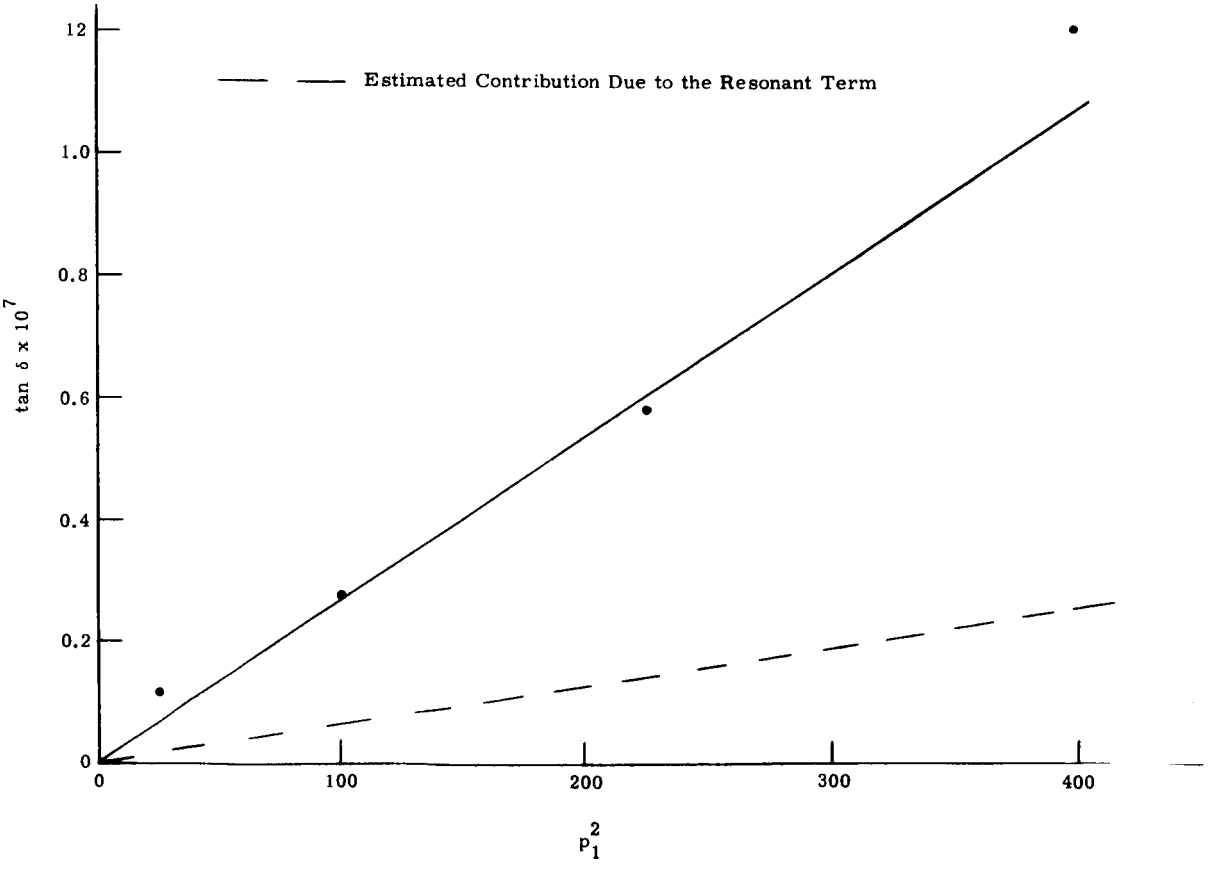

Figure 10. Tan δ versus p_1^2, ν = 169.794 Gc

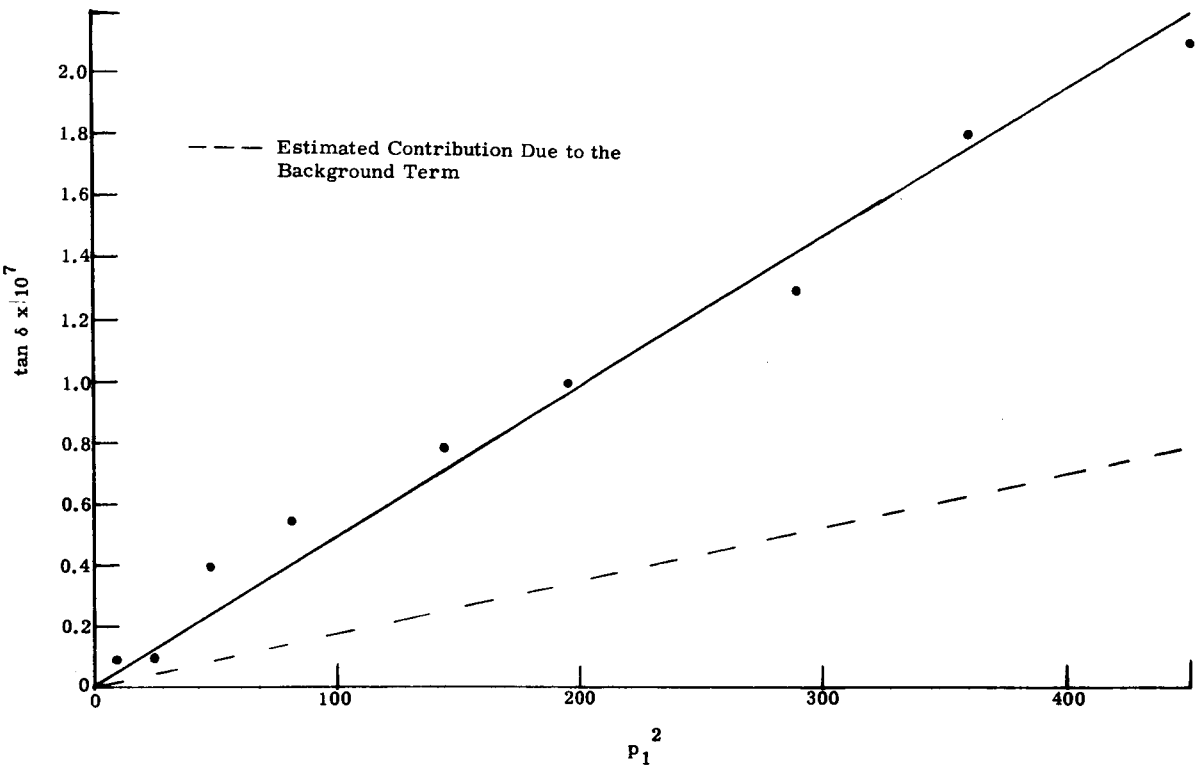

Figure 11. Tan δ versus p_1^2, ν = 190.000 Gc

Figure 12 gives a plot of tanδ for fixed values of p_1 and p_2 as a function of frequency. Using Equation (16), k_{12}^W could be determined to be 18 Mc/mm.

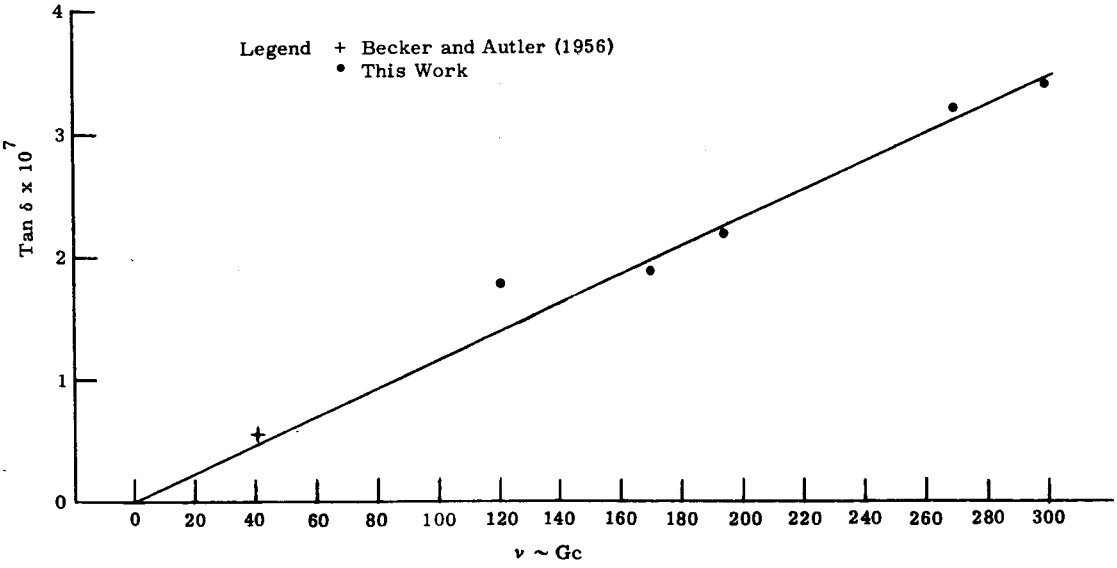

Figure 12. Tan δ' versus ν, p_1 = 15 mm, p_2 = 800 mm of N_2
(See Equation 16)

Two groups of data were taken for the determination of k^o_{12} with N_2 in order to detect any deviations from the assumed shape factor. One group of measurements was made at fixed frequencies approximately 100 to 200 Mc from the center of the line at 183.31 Gc using values of p_1 of 1 to 2 mm and up to 300 mm of the foreign gas. In these data $\tan\delta_{max}$ was used to determine the exact pressure of H_2O by means of Equation (18a) since this way of determining small pressures was found preferable to the Dubrovin gauge. Using the attenuation by pure H_2O measured as the first point of each set of measurements in this group, k^o_{11} was carefully determined as well as k^o_{12} which is independent of p_1. Figure 13 shows typical curves of $\tan\delta$ versus the $\log_{10}$ of p'_0.

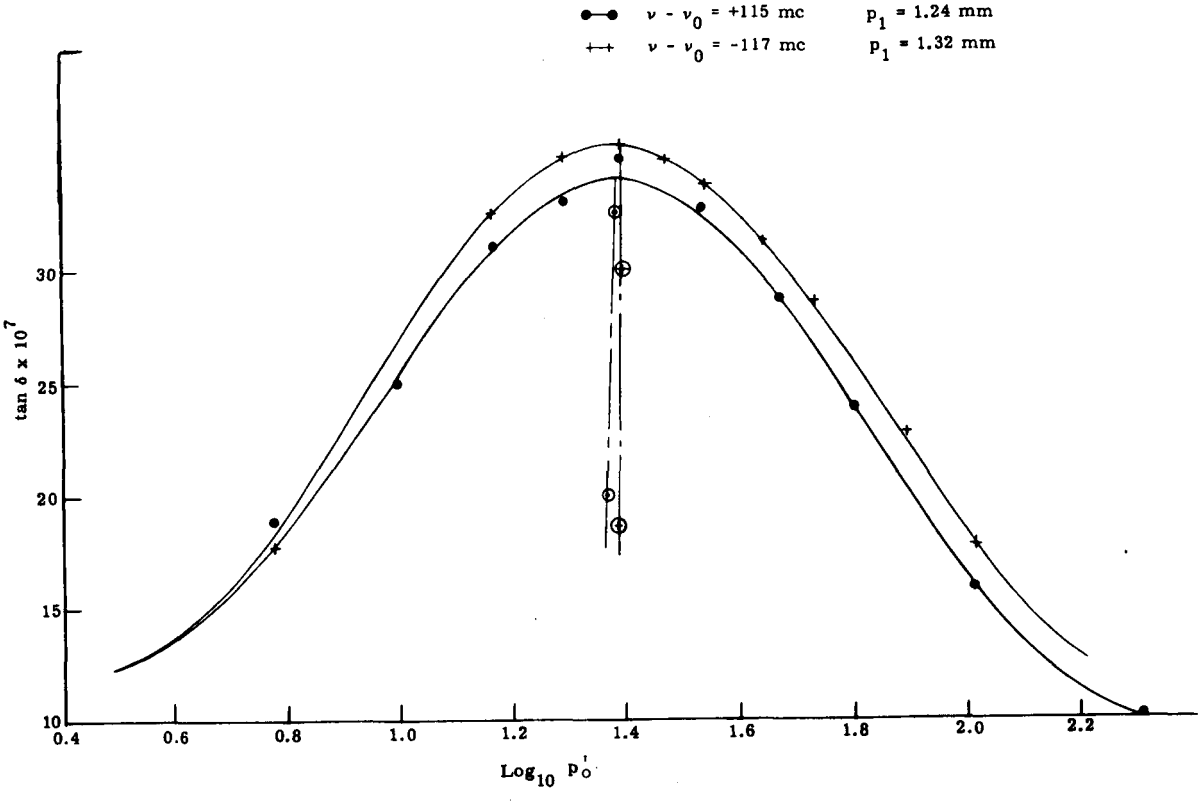

Figure 13. Tan δ versus Log p' for N_2, T = 300°K

The second group of measurements was made at frequencies between 1 and 3 Gc from line center and here corrections for the background were necessary. On the other hand, the partial pressures of H_2O used in this region (15mm) could be determined accurately and the line strength could be compared to theory. Figure 14 shows a set of data together with the background corrections.

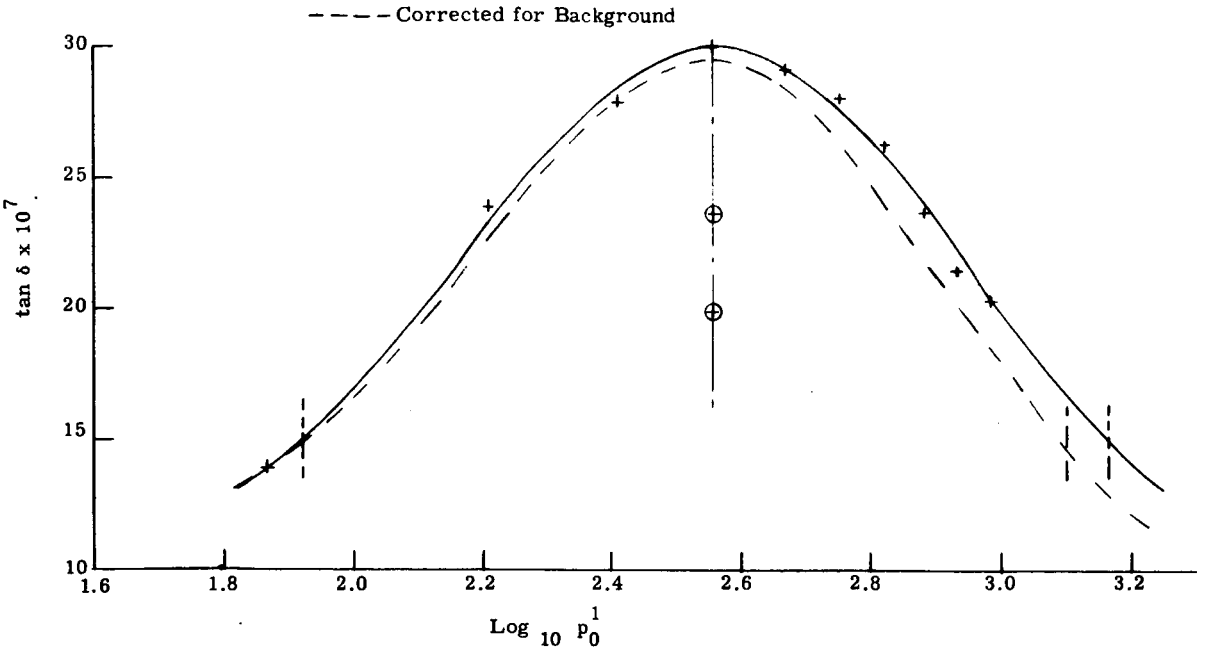

Figure 14. Tan δ versus Log p' for N_2, $\nu - \nu_0$ = 1.5 Gc, T = 300°K, p_1 = 15 mm

Tables Ia and Ib give summaries of results in these two groups:

TABLE Ia

Results for Group 1 Measurements
(100 to 200 Mc from the Line Center at 183.31 Gc)

$\nu_{Gc} - \nu_{01}$	p_1 (mm/Hg)	k^o_{12} Mc/mm	k^o_{11} Mc/mm	k^o_{11}/k^o_{12} Mc/mm	$\tan\delta_{max}$ Percent	$\Delta_{\frac{1}{2}} \log (p'_0)$*
+0.310	2	4.7	21	4.5		1.23
+0.180	1	4.8	30	6.2		1.17
+0.110	½	(4.3)	24	(5.6)		1.20
+0.110	1	(4.6)	25	(5.0)		1.20
+0.115	1	4.6	24	5.2		1.21
+0.115	1	(4.7)	25	(5.3)		1.18
-0.210	1	4.7	24	5.1		1.15
-0.170	2	4.7	19	4.0		1.00
-0.182	2	(4.3)	28	(6.5)		1.30
-0.117	1	4.7	22	4.7		1.25
<		4.7	24	5.0		>

TABLE Ib

Results for Group 2 Measurements
(1 to 3 Gc from the Line Center at 183.31 Gc)

-2.7	10	4.0	21.0	5.2	97	1.14
-2.7	16	4.1	24.5	6.0	91	1.00
+2.3	10	(4.3)	(17)	(4.0)	98	1.04
+2.3	15	4.3	24	5.6	98	1.00
+3.0	18	4.3	19	4.4	119	0.9
+1.5	14	3.9	21.7	5.6	100	1.02
<		4.1	22.0	5.4	100	1.02 >

* This column gives the 1/2 amplitude width of the tanδ versus $\log_{10} p$ curves in units of $\log_{10} p$.

The sixth column gives the value of $\tan\delta_{max}$ in terms of a percent value compared to theory. In Table Ia this column is left blank since 100 percent agreement was assumed. The values in parentheses were adjusted on the basis of the corrections that had to be applied to p_1 and are not counted in the averages in the bottom rows.

It is not possible to ascribe the difference between k^o_{12} as measured in group 1 and group 2 experiments definitely to the lineshape since an experimental error of ±5 percent can not be excluded. For the present these values will be averaged in the overall results in Table II.

TABLE II

Linewidth Parameters in Mc/mm

	H_2O	N_2	CO_2	O_2
k^o_{11}	22 ± 2	-	-	-
k^w_{11}	200 ± 40	-	-	-
k^o_{12}	-	4.4 ± 0.2	6 ± 0.3	2.7 ± 0.2
k^w_{12}	-	19 ± 2	65 ± 7.0	-

Figure 15 gives the absorption calculated by Equation (1b) using these values over the range from 10 to 300 Gc.

E. RELIABILITY OF THE DATA AND LIMITATIONS OF THE APPARATUS

In this section, various limitations of the apparatus will be discussed and the effect these limitations have on the reliability of the data which have been reported. The factors limiting the reliability of the data may be divided into several groups. In each group errors can be assessed by independent experiments. The groups to be considered are:

1 Pressure measurements

2 Q measurements

3 Stability of components over the period of a measurement

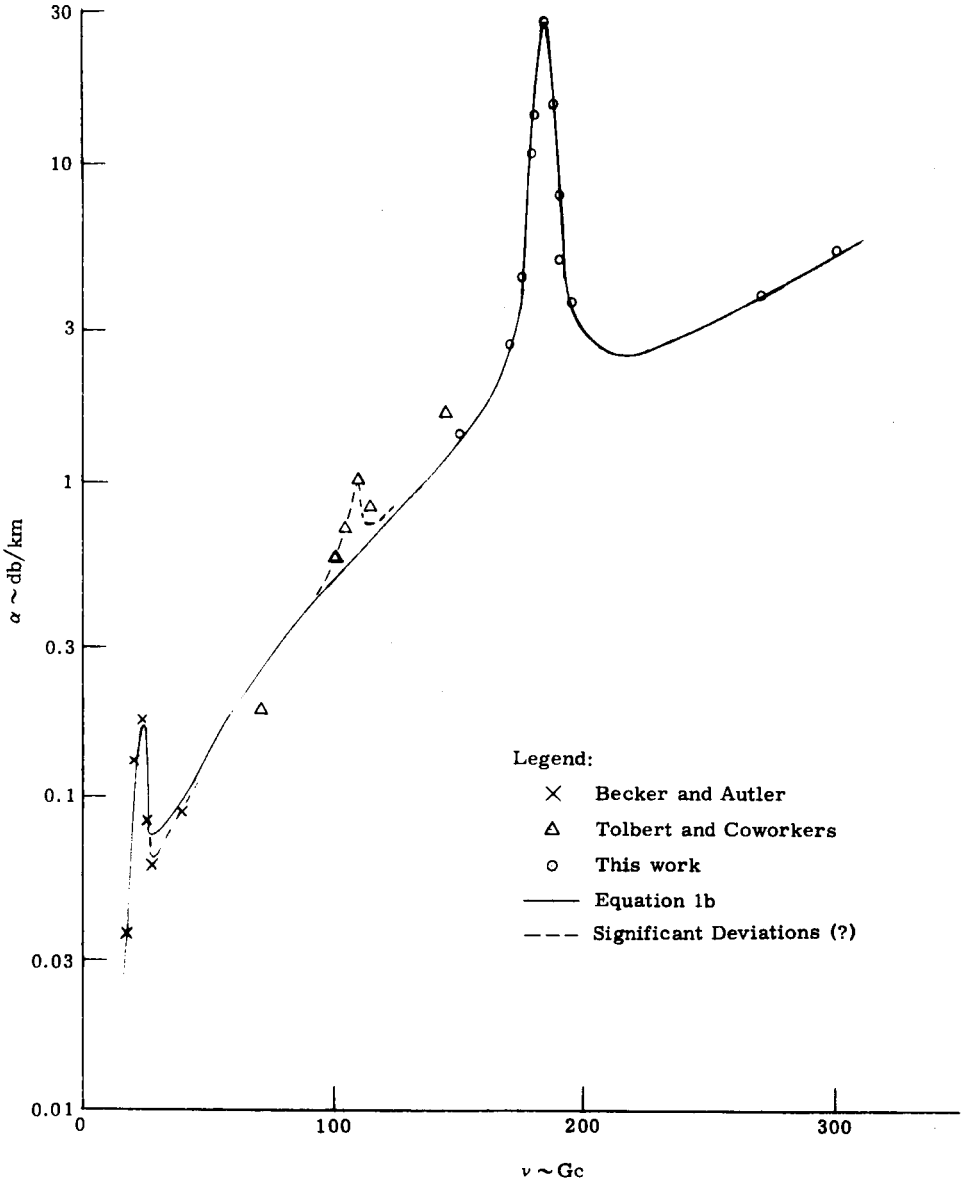

Figure 15. Absorption Coefficient α Due to 7.5 mm of H_2O in 750 mm of N_2 versus Frequency ν

4 Stability of the cavity and its windows

5 Frequency measurements

6 System linearity

7 Gas purity.

1. Pressure Measurements

Pressures in the range from 0 to 20 mm of Hg were read on a Dubrovin gage having a linear scale from 0 to 20 mm graduated in linear increments of 0.2 mm. The gage was calibrated at its upper limit against a mercury manometer and against a quartz Bourdon-tube at 5 and 10 mm. The Bourdon gage was unfortunately not available during the experiments and the Dubrovin gage could not be relied on at low pressures where gradual shifts in the zero reading and sticking created an uncertainty in the order of 0.3 mm of Hg. As explained in the text, it was, therefore, necessary to rely on calculated line strength to determine the pressure of H_2O below about 5 mm of Hg. This limitation prevented the accurate investigation of line shapes near the line center and generally imposed a limitation of about 3 percent on the measurements of k_{11}^{o} and $\tan_{max}\delta$. It is entirely probable that a number of interesting features of the $\tan\delta$ versus log p curves are masked by this uncertainty.

2. Q Measurements

Q measurements are needed in both methods (Q and amplitude) and must be made before each series of measurements. In general, it was possible to measure the frequency interval between 1/2 power points repeatedly to about ±3 percent. However, the values obtained varied sensitively with coupling changes that occurred as a result of mechanical operations made on the cavity, either in intentional adjustments or during pressurization. These changes often amounted to ±15 percent of the initial set of readings. It is very doubtful that such large changes actually occurred during a measurement series or that they were systematic enough to affect the average results of repeated measurements by more than 5 percent. The origin of the sensitivity to mechanical influences lies primarily in the relatively tight coupling into and out of the cavity. As more power becomes available a higher insertion loss and less coupling is feasible. The value of Q affects measurements of line strength but not the values of k.

3. Stability of Components

The stability of power generating and transmitting components as well as that of detectors and multipliers imposes limitations on the ultimate sensitivity of the apparatus. In principle, it is possible to read the amplitude of the cavity response curve on the oscilloscope to better than 0.2 percent. This value at a Q_0 of 330,000 represents a value of $\tan\delta$ given by

$$\tan\delta = \frac{1}{Q_0} \times \sqrt{\frac{100.2}{100}} - 1 \approx 3 \times 10^{-8}$$

To utilize this sensitivity requires that power generating, transmitting and detecting components must have stabilities in the same order. In general, this is not the limiting factor since the changes in Q and transmission resulting from pressure changes in the cavity cause larger fluctuations. For some self-broadening measurements at very low pressures, where losses are small and the Q is stable, stability of components become important. It was possible to achieve the required high degree of stability for each measurement only after days of painstaking efforts and improved mm-wave components would open the way for a number of interesting investigations.

4. Stability of the Cavity and its Windows

The most severe limitations upon sensitivity and precision were imposed by changes in insertion loss as a result of mechanical deformation of the cavity, the tuned coupling arrangements and the windows. When a loss - less gas (He or N_2) was admitted to the cavity, both arbitrary and systematic changes in transmission occurred. Such changes generally amounted to 2 percent of the initial transmission or to an apparent loss given by

$$\tan \delta \approx \pm 3 \times 10^{-7}$$

the values of tan δ at these pressures during measurements of k_{12}^{Q} were of the order of 30×10^{-7} so that 10 percent errors were generally expected. These errors, however, were not systematic, so that they could be averaged out.

A more serious problem occurred during the measurement of k_{12}^{W}, where the tanδ was of the order of 1 to 3×10^{-7}. Here the errors in each measurement could exceed the measured quantity and it became necessary to make special and laborious efforts to stabilize the cavity and to eliminate the arbitrary changes in transmission. The remaining systematic changes with pressure were taken care of by calibration.

5. Frequency Measurements

The denominators of the first two terms in Equations (10 and 11) depend on $(\nu - \nu_0)$ and near resonance this is a critical quantity. Frequency could be measured to 1 cps in 10^8 cps. The smallest value of $(\nu - \nu_0)$ used was 0.1 Gc or 0.1 in 200 compared to ν_0. Frequency measurements therefore imposed no limitation in this work.

6. System Linearity

System linearity was carefully checked by attenuating the power supplied to the cavity by known amounts and observing the cavity response on the

scope. The attenuator was in turn calibrated independently at various power levels. In addition to these checks the use of the amplitude and Q methods as a cross check over a power range of 18 db eliminated the possibility of gross error.

7. Gas Purity

Two sources of error are to be considered under this heading – the purity of the water vapor and that of the foreign gases used.

The vacuum system was not built for high vacua and the improvised tunable couplings often caused minor leaks. The water vapor, therefore, frequently contained some air. This problem could be controlled by flushing the system with H_2O vapor before a critical experiment. To check whether a given charge in the cavity was sufficiently pure, a gas sample was compressed in a McLeod gage and the residue measured.

Critical measurements with foreign gases presented more of a problem. Thus, it was necessary to ascertain that 800 mm of a foreign gas did not contribute a loss to the very small loss expected in wing measurements. To check this point 800 mm of the gas were admitted while observing the amplitude of the Q curve. This invoked all the problems enumerated under 4 as well as possible changes in transmission due to the retuning of the mirrors. (The mirrors were retuned to compensate for the dielectric constant of the gas.) Of the gases used, only CO_2 had any measurable loss at 300 Gc. This loss was presumably attributable to the induced absorption due to the quadrupole moment of the CO_2 molecule. In measurements with CO_2 the loss due to the CO_2 in the cavity had to be subtracted from the losses measured for the mixtures.

F. DISCUSSION

In discussing the measurements reported here and in comparing them to other work, it is necessary to restrict oneself to a consideration of those efforts that were specifically directed at the linewidth parameters in the microwave region. The constants k^o_{12} and k^o_{11} were measured in an absorption cell at very low pressures by Rusk (1965). He found the values k^o_{12} = 3.78 and k^o_{11} = 19.1 for N_2 and H_2O, respectively, for the line at 183.31 Gc. Becker and Autler, using a nonresonant cavity near the 22.3 Gc line at much higher pressures found nearly the same values (k^o_{12} = 3.58, k^o_{11} = 14). In addition their data in the wings may be interpreted as indicating a $k^o_{12} \approx 18$, as pointed out by Van Vleck. One can in fact pursue the matter even further and derive from their data a figure for k^w_{11}. The experiments of Becker and Autler were conducted at two partial densities of H_2O, 10 gr/meter^3 and 50 gr/meter^3 and it was noted that the wing absorption at the low density re-

quired a background term four times as high as calculated on the basis of k^{o}_{12} = 3.6 Mc/mm and at the high density a factor of 6 was required to reconcile theory and experiment. Assuming that their observations are due to k^{w}_{11} we find thus that 40 mm of H_2O are approximately one half as efficient as 750 mm of N_2 so that, very approximately

$$k^{w}_{11} \approx 1/2\, k^{w}_{12}\, \frac{750}{40} \simeq 130 \text{ Mc/mm}$$

A more precise calculation, taking into account the values of k^{o}_{12} for N_2, O_2 and the effective pressures of the various mixtures involved gives a value for k^{w}_{11} of 140 Mc/mm.

The general features emerging from this and earlier work are thus in no doubt. They may be summarized as follows: Near the microwave absorption lines the lineshape is Lorentzian and also consistent with the theory of Van Vleck and Weisskopf. The linewidths for self-broadening and for foreign gas broadening are here in close agreement with the Anderson (1949) (Reference 25) theory as calculated by Benedict and Kaplan (1959) (Reference 19). In the wings of the lines, on the other hand, the absorption is substantially larger than predicted by these theories but can be reconciled with the lineshape theory of Van Vleck and Weisskopf on the assumption of much larger linewidth parameters than those found near the line centers. For pure H_2O vapor, in particular, this parameter reaches the enormous value of 200 Mc/mm.

There is a suggestion in the data that the value of k^{o} for a given mixture may be empirically related to the corresponding value of k^{w}. Thus, it may be seen from Figure 16 that the total absorption in the center of the lines is approximately independent of the mixture used; this is true even for a hypothetical broadener similar to H_2O in its characteristics. It should be noted that this independence is true only at one pressure of the broadener since the background and the line depend, respectively, linearly and inversely on the values of $p'k^{o}$ and $p'k^{w}$. For any two systems it is therefore always possible to find a pressure at which the peak absorptions of a given line will be equal. Whether the peak absorption for all other broadeners will then also have the same value or whether this apparent isometry is purely accidental is an open question inviting some further work.

It is probable that there exists a transition region where the theoretical line shape breaks down and where the linewidth parameter loses its meaning. It is not the purpose of the present report to examine this matter further but it seems a challenging task in view of the fact that the integrated absorption of a given gas mixture must obey certain dicta of spectroscopic stability.

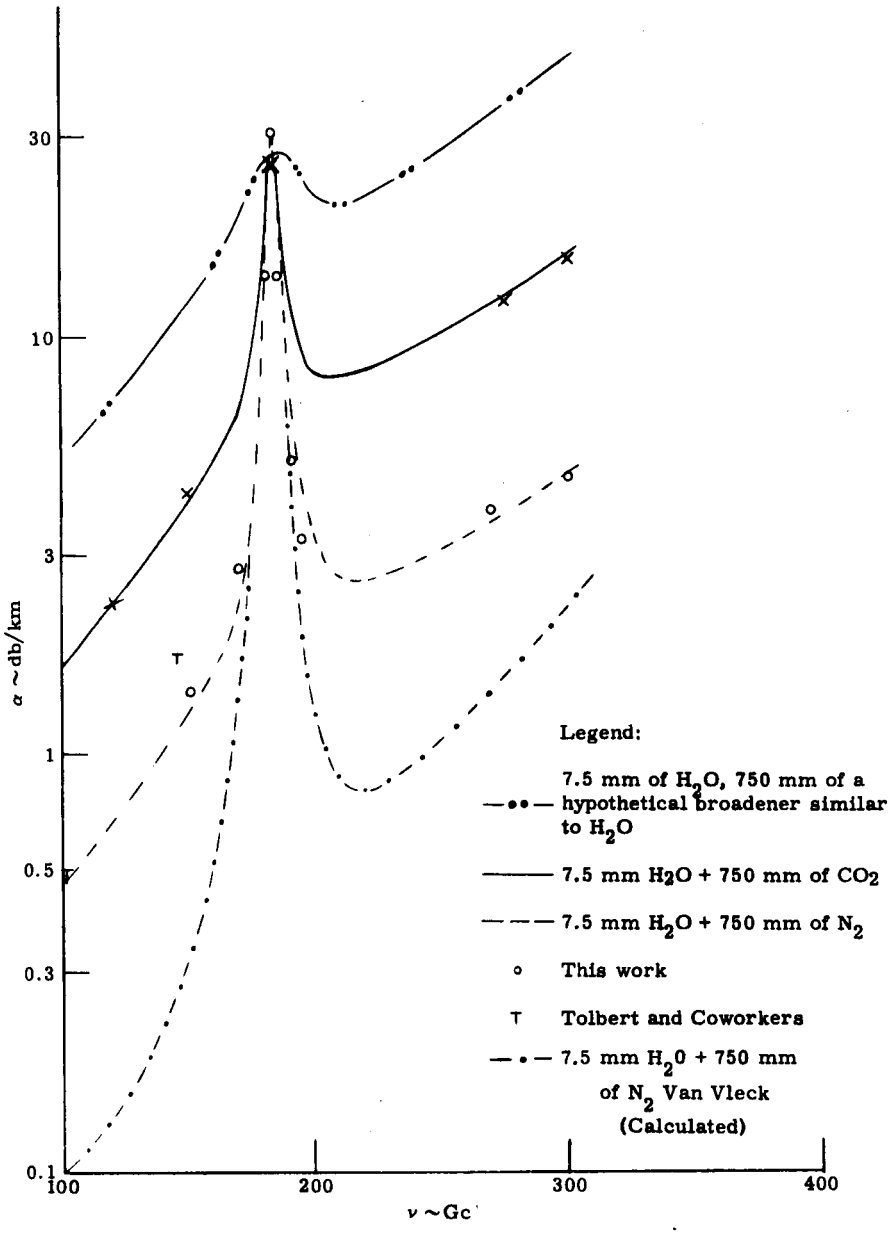

Figure 16. Absorption Coefficient α for Various Gas Systems, p_1 = 15 mm, p_2 = 750 mm

It remains only to compare group 1 and group 2 results for the line at 183.31 Gc to each other and to the results of Rusk. This is done in Table III.

TABLE III

Comparison of Linewidth Parameters at 183.31 Gc

	Rusk	Group 1	Group 2
k^{o}_{12} (Mc/mm)	3.8 ± 5%	4.7 ± 0.3	4.1 ± 0.3
k^{o}_{11} (Mc/mm)	19.0 ± 5%	24 ± 2	22 ± 2

In view of the large difference in pressure under which these measurements were made it is probably more profitable to emphasize the agreement in the data rather than their differences. Here again the conclusion is inevitable that the line shape theory is adequate to describe absorption near transitions, and that, provided the background is subtracted out, the same linewidth parameter serves all experimental conditions.

III. LOSS MEASUREMENTS ON O_2

A. INTRODUCTION

There have been indications in the literature (References 14 and 15) that anomalies observed in the atmospheric absorption between 110 to 140 Gc may be due to an interaction of H_2O on O_2 near the oxygen absorption line at 118.75 Gc. At present, the capabilities of the resonant cavity do not permit measurements in the wing region of this line but an anomalously large effect in the wings should also result in an excessive broadening near the line center where the sensitivity of the cavity is adequate.

B. EXPERIMENTAL METHOD AND RESULTS

In these experiments another technique was found expedient which permitted the evaluation of the effect of H_2O on O_2 in terms of that of N_2 and of the self-broadening of O_2.

The cavity was tuned to 118.760 Gc and the attenuator adjusted for a full response on the oscilloscope screen. Ten millimeters of O_2 were then admitted into the cavity and the amplitudes of the attenuator were read. Ten millimeters of H_2O, N_2, or O_2 were then added and the amplitudes were again read. Using Equation (18) at $(\nu - \nu_0) \approx 0$ gives

$$\tan\delta = p_1 C_{01}^t \frac{\nu_0}{p_0' k_{12}^o} \tag{20}$$

where the subscript 1 refers to O_2

For pure O_2, $k_{12}^o = k_{11}^o$ and $p_0' = p_1$ so that,

$$\tan\delta = C_{01}^t \frac{\nu_0}{k_{11}^o} \tag{20a}$$

This is independent of pressure so that the amplitude does not change. This step was used to check on the instrument's performance in this series

of tests. For N_2, it has been shown by Artman (Reference 26) that $k^o_{11} \approx k^o_{12}$ so that from Equation (12a)

$$p_0' \approx p_1 + p_2 \tag{21}$$

and therefore, on adding 10 mm of N_2 to 10 mm of O_2

$$\tan\delta = C^t_{01} \frac{\nu_0}{2\, k^o_{11}} \tag{21b}$$

so that the loss now is cut in half. This, too, was used as a check.

When 10 mm of H_2O were added to 10 mm of O_2, the amplitude dropped by the same amount, indicating that the cross section for H_2O collisions with O_2 is not significantly larger than that for the other two gases.

C. NEED FOR ADDITIONAL WORK

As is well documented in the literature (Reference 27) the absorption line at 118.75 Gc of O_2 is of a magnetic origin and the oxygen molecule which has only a weak quadrupole moment can not be expected to interact strongly with the electric dipole on H_2O. The above result is, therefore, not surprising, and further work is required to determine the origin and nature of the anomaly which has been reported.

IV. SPECTROSCOPIC INVESTIGATION

A. INTRODUCTION

The purpose of spectroscopic efforts in this program is to provide information about the energy levels and transitions in the molecules which contribute to atmospheric absorption. Together with the information on linewidth at atmospheric pressure obtained in the resonant cavity, such data provide means for calculating losses at frequencies not yet reached and at points of the spectrum in between those at which measurements have been taken.

Efforts were concentrated on three molecules: O_2, H_2O, and NO_2. To date, these efforts are not sufficiently advanced to provide comprehensive new details on these systems. The salient features of the spectra of these molecules and the status of the work will be described below.

B. SEARCH FOR ROTATIONAL LINES IN O_2

As pointed out in Chapter III, Section C, the O_2 molecule has no electric dipole and its spectrum in the millimeter region consists primarily of transitions in which the electronic spin alignment with respect to the total orbital angular momentum changes by one unit. These transitions lie in a band about 60 Gc except for one line at 118.75 Gc and have been extensively studied. (References 2 and 3.)

Because of the perturbation of the wave functions of O_2 by the electron spin, the orbital angular momentum N of the molecule is not a good quantum number and $\Delta N = 2$ transitions between the levels usually denoted by N+, o, - are possible (Reference 28). Mizushima (Reference 29) has predicted three such transitions (Table IV).

The intensity of the strongest one of these lines ($1_+ \rightarrow 3_-$) is given by him as roughly 10 times the intensity of the ($1_+ \rightarrow 1_0$) line in the magnetic spectrum. This would still make it a relatively weak line* and in view of the small amount of power available at that frequency, special efforts must

* The absorption at the peak of these lines would be comparable to the losses in the gaps between the H_2O absorption lines.

TABLE IV

Rotational Transitions Predicted in O_2

Transition	Frequency in mc	Relative Strength
$1_0 \rightarrow 3_-$	368,447	0.55
$1_+ \rightarrow 3_-$	424,613	9.12
$1_+ \rightarrow 3_0$	487,199	7.94

be made in the search for it. For one thing it is advantageous to cool the cell; secondly, since the O_2 molecule is magnetic, Zeeman modulation and synchronous detection may be employed. The search for this line was, therefore, made in an existing absorption cell which had provisions for cooling and Zeeman modulation. A number of problems developed particularly in connection with cooling, such as condensation on the windows and an inconveniently high consumption of coolant. These difficulties made the use of this particular cell very tedious. In addition, calculations showed that the predicted strength of the line would make a longer cell desirable.

Since the effort on O_2 competed for men and materials with more important and promising investigations on H_2O, it was decided to postpone this phase of the work until a new cell could be made available.

C. THE H_2O MOLECULE

1. Line Positions

H_2O is an asymmetric top molecule which has only a few lines in the millimeter region. In between these lines lie the "windows" in the atmosphere and a complete knowledge of the molecule is, therefore, desirable.

Two lines have been observed previously in the microwave region; these are the $5_{-1} \rightarrow 6_{-5}$ transition at 22,235.1 Mc and the $2_2 \rightarrow 3_{-2}$ transition at 183,310.0 Mc. These resonances and the ones extending into the shorter wavelength region were predicted from infrared data. Since the energy values of these states have only small separations, the resonances in the microwave and millimeter regions cannot be predicted with precision from infrared data.

The energy level differences calculated from the infrared data by Benedict, et al (References 30 and 31) give predicted values to three significant figures. Values given by other investigators do not attain this accuracy.

The predicted and the observed resonances, which occur in the microwave and millimeter regions, are listed in Table V, together with their intensities. Only the strongest of the allowed transitions are listed.

TABLE V

Predicted and Observed Transitions in H_2O Below 600 Gc

Transition	Predicted Frequency (Gc)	Intensity	Observed Frequency (Gc)
$5_{-1} \rightarrow 6_{-5}$	22.2	9.290×10^{-3}	22.235
$2_2 \rightarrow 3_{-2}$	183.6	4.675×10^{-2}	183.310
$*4_0 \rightarrow 5_{-4}$	325.5	5.826×10^{-2}	325.153
$*3_1 \rightarrow 4_{-3}$	379.8	1.726×10^{-1}	380.196
$5_5 \rightarrow 6_1$	439.4	1.381×10^{-2}	
$6_5 \rightarrow 7_3$	442.2	2.835×10^{-3}	
$*3_3 \rightarrow 4_{-1}$	449.0	1.714×10^{-1}	448.000
$5_4 \rightarrow 6_2$	468.0	1.572×10^{-2}	
$4_4 \rightarrow 5_0$	474.5	6.529×10^{-2}	
$1_1 \rightarrow 1_{-1}$	556.9	1.083×10	

* Resonances observed during this report period

The new lines found in this report period were observed from the following harmonics of the fundamental frequencies:

5th and 6th of 76,039.6 and 63,366.3, respectively
6th and 7th of 74,666.8 and 64,000.0, respectively
5th and 6th of 65,030.7 and 54,192.1, respectively

From the table, it is seen that the $1_1 \rightarrow 1_{-1}$ transition is the strongest in intensity and should be observable once power is attained in the 550 to 560 Gc region. With the possible exception of the $6_5 \rightarrow 7_3$ transition, the other transitions not yet observed should be observable with sufficient power in the regions of interest. At one point during this investigation the 510 Gc line of OCS was observed at the seventh harmonic of 72,922 Mc in a video presentation.

2. Stark Effect on H_2O

The Stark effect was observed on three of the microwave lines. The Stark cell was of the conventional type with center septum located such that only $\Delta M = 0$ transitions occurred; i.e., the electric vector of the microwave field was parallel to the electric vector of the Stark field. The 325 Gc and 448 Gc lines have not been observed through the Stark cell as yet. The 325 Gc line is weak in intensity, and sufficient power was not attained for the stronger 448 Gc line. Both of these lines were evidently attenuated too strongly in the conventional Stark cell. A new Stark cell has been constructed employing a split waveguide, thereby eliminating the center septum. With this type of construction, the electric vector of the microwave field may be perpendicular to the vector of the Stark field resulting in $\Delta M = \pm 1$ transitions or it may be used for $\Delta M = 0$ transitions. If the transitions are not attenuated too strongly in this type cell, it will be possible to detect some of the weak predicted lines by a Stark modulation detection system.

Second order Stark effects are generally applicable to the asymmetric rotor. The entire Stark energy is given as: (Reference 32)

$$W_{J\tau M} = \sum_{x=a,b,c} \frac{\mu_x^2 E^2}{2J+1} \sum_{\tau'}' \left[\frac{J^2 - M^2}{J(2J-1)} \frac{{}^xS_{J\tau,\, J-1\tau'}}{W^o_{J_\tau} - W^o_{J-1_{\tau'}}} + \frac{M^2}{J(J+1)} \frac{{}^xS_{J\tau J\tau'}}{W^o_{J_\tau} - W^o_{J_{\tau'}}} + \frac{(J+1)^2 - M^2}{(J+1)(2J+3)} \frac{{}^xS_{J\tau,\, J+1\tau'}}{W^o_{J_\tau} - W^o_{J+1_{\tau'}}} \right] \qquad (22)$$

where $\sum_x$ takes into account each component of the dipole moment along the principal axis of inertia; $W^o_{J_\tau}$ represents the unperturbed energy of the rotational state designated by J_τ; ${}^xS$ values are tabulated sums of the dipole matrix elements, and $\sum'_{J_{\tau'}}$ is taken over all states except J_τ.

For the asymmetric species, H_2O in particular, the dipole moment is along the b axis; thus, allowing b type transitions to be the most predominant. Equation (22) is then calculated for the dipole moment along the b axis. This Stark energy for the asymmetric species has the general form

$$W_{J_\tau M} = \left(A_{J_\tau} + B_{J_\tau} M^2\right) E^2 \qquad (23)$$

For the asymmetric species under consideration, the selection rules on $K_{-1}K_1$ from King, Hainer and Cross are the following: ee $\leftrightarrow$ oo and eo $\leftrightarrow$ oe, where o and e stand for odd and even, respectively. The subscript τ is obtained from the relation: $\tau = K_{-1} - K_1$.

The data on the Stark effect (Figures 17 and 18) have not yet been fully evaluated and will not be reported here. Critical evaluation is necessary because of the uncertainties in the theoretical line strength due to the distortion of the molecule.

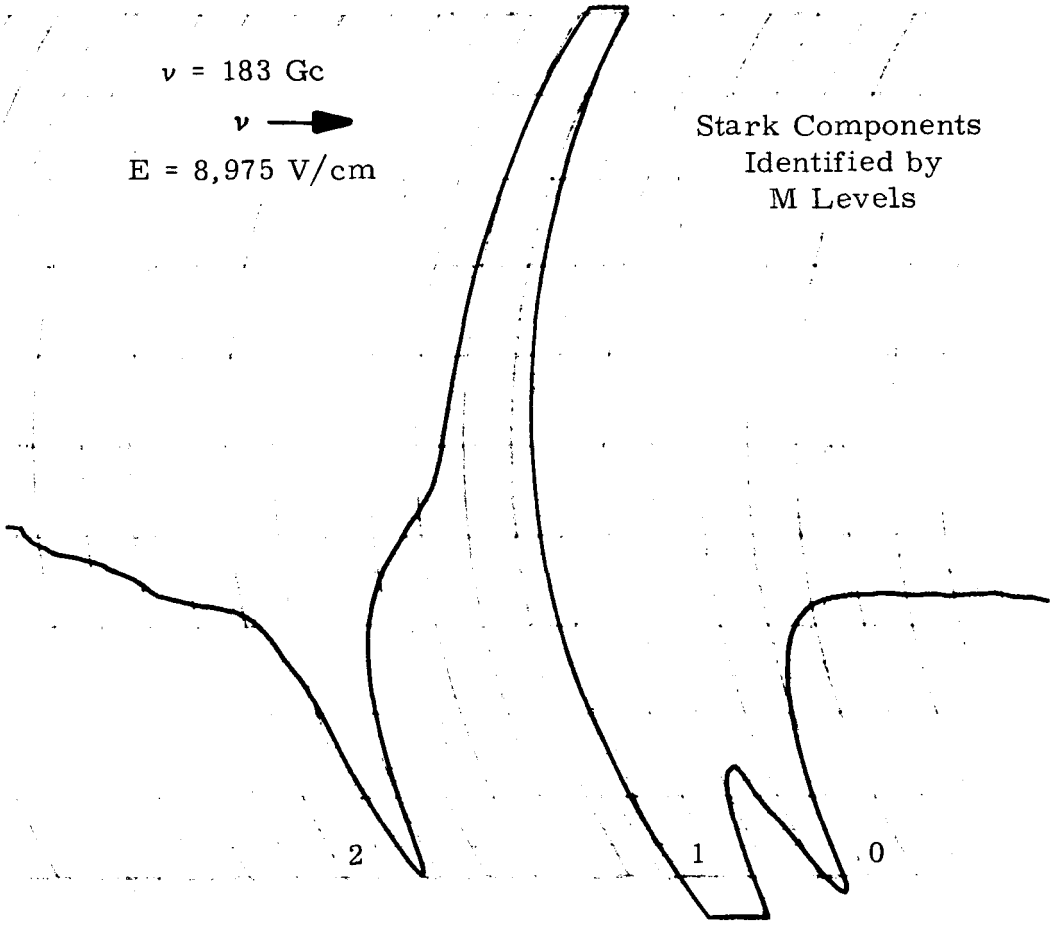

Figure 17. Stark Effect in H_2O at 183 Gc

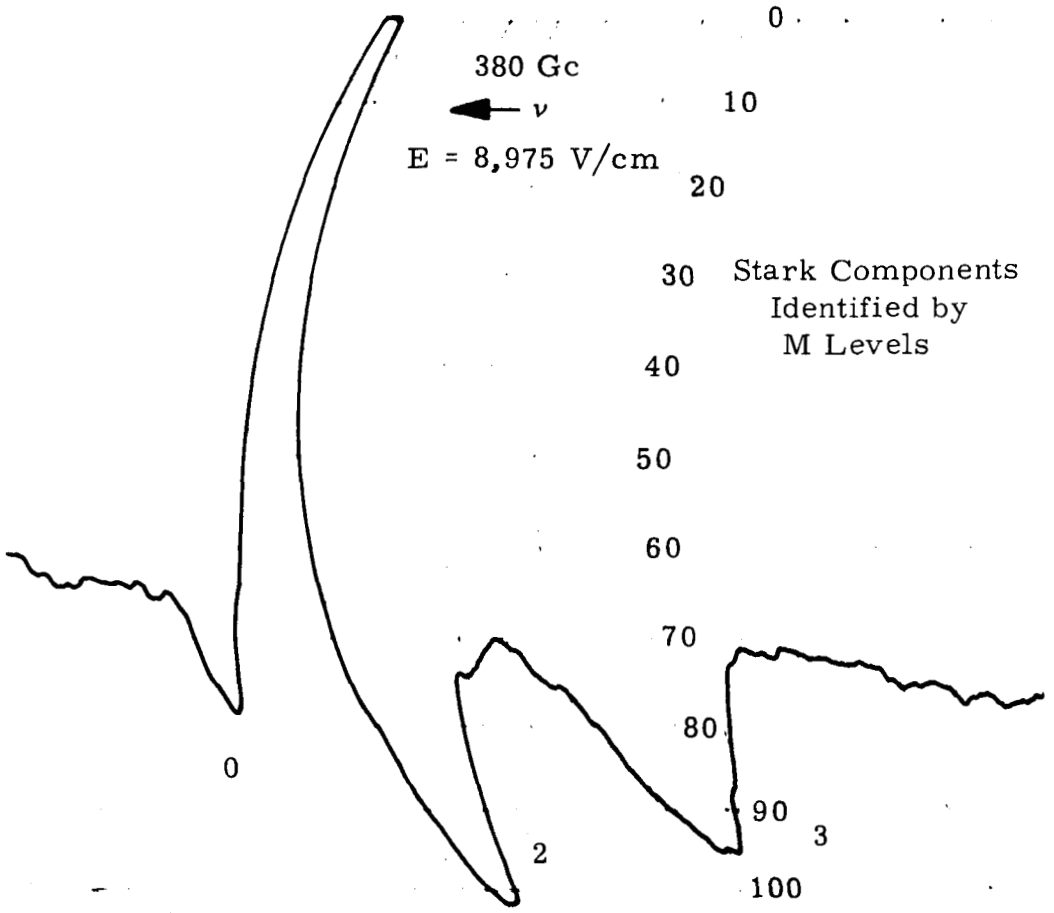

Figure 18. Stark Effect in H_2O at 380 Gc

D. NO_2

The NO_2 molecule is an asymmetric top with one unpaired electron. The unpaired electron spin interacts with the nuclear spin on (N^{14}) to give a hyperfine structure (Reference 33). NO_2 is found in the upper atmosphere and is, therefore, of some interest. A number of lines not previously reported in the literature were found but no final assignments have been made. This work is progressing as a continuing effort and will require further experimental and theoretical study. To date the following series of lines have been cross checked from two different fundamental frequencies (Table VI).

TABLE VI

Transition Tentatively Assigned to NO_2

235,055.5 Mc	215,269.8 Mc
235,030.6 Mc	215,262.9 Mc
235,077.6 Mc	215,255.5 Mc
235,510.2 Mc	215,246.6 Mc
	215,243.3 Mc
	215,236.4 Mc
	215,075.7 Mc

V. CONCLUSIONS AND RECOMMENDATIONS

Planetary atmospheres are highly variable in content and physical state and it would seem that data of a general nature, which permit the prediction of propagation characteristics under specific conditions and for a variety of molecular species, are as important for many problems as the actual absorption measurements are at ground level.

From the absorption measurements on H_2O, there is a strong indication that the "windows" in atmospheres are not nearly as transparent as one might be led to believe from measurements on absorption lines at low pressures. This effect may be due to the deviation of line shapes from theoretical models, or, perhaps, because of the formation of complexes in which large numbers of lines could occur. Specific examples of induced non-resonant absorption in CO_2 and other non-polar gases have been reported by Maryott and Birnbaum, (Reference 34) and Heastie and Martin (Reference 35) have measured losses in the far infrared (30-100 cm^{-1}) in N_2. Gebbie and Stone (Reference 36) observed the rotation spectrum of CO_2 due to the induced dipoles at high pressures.

It is likely that small quantities of polar gases in some planetary atmospheres would cause very substantial losses and the effects of polar upon non-polar gases is bound to result in some interesting phenomena.

At present, there is considerable emphasis on covering the range to 1000 Gc as quickly as possible. It would seem that the problems mentioned above should receive equal attention. In fact, the region above 500 Gc is difficult because no suitable sources exist and at the same time, the feasibility of attacking practical problems such as communications in this region depends on such sources also. The exploration of this region need not proceed any faster than the capability of utilizing it, particularly since there are many interesting and important problems on the sidelines.

In the pursuit of higher frequency non-resonant measurements, problems arise in connection with instrumentation. Since spectroscopy is not the prime purpose of the suppliers of hardware for the submillimeter region, available equipment, power supplies for instance, are not of a suitable quality and require redesign. The absorption cells, interferometers and components for each new frequency range require considerable modification,

redesign, and sometimes special techniques and processes. These considerations lead to the conclusion that the speed of progress of the physical measurements is closely related to the availability of supporting programs dealing with hardware and components design and evaluation.

It is therefore, recommended:

1 That the program goals be broadened to include some of the interesting and mission related phenomena which can be pursued with existing means such as induced absorption and absorption in mixtures of polar gases.

2 That the institution of related supporting programs in this laboratory be considered. Such programs should provide for the construction and acquisition of sources, instruments, and components necessary for obtaining quantitative monochromatic absorption data in the region from 500 to 1000 Gc.

REFERENCES

1. B. Bleaney and R. P. Penrose, Nature 157, 339 (1946); Proc. Roy. Sec. A89, 358 (1947)

2. R. T. Weidner, Phys. Rev. 72, 1268 (1947)

3. W. Gordy, Rev. of Mod. Physics 20, No. 4, October 1948

4. W. Culshaw, IRE Trans. on Microwave Theory and Techniques, page 182, March 1960

5. W. Culshaw, IRE Trans. on Microwave Theory and Technique, page 135, March 1961

6. W. Culshaw, IRE Trans. on Microwave Theory and Technique, page 331, September 1962

7. R. W. Zimmerer, IRE Trans. on Microwave Theory and Technique, page 371, September 1963

8. M. Lichtenstein, J. J. Gallagher and R. E Cupp, Review of Scientific Instruments, Vol. 34, No. 8, August 1963

9. A. G. Fox and Tingye Li, Bell System Technical Journal, page 453, March 1961

10. G. D. Boyd and J. P. Gordon, Bell System Technical Journal, page 489, March 1961

11. G. D. Boyd and H. Kogelnik, Bell System Technical Journal, page 1347, July 1962

12. J. H. Van Vleck and V. F. Weisskopf, Rev. Mod. Phys. 17, 913, 1945

13. J. H. Van Vleck, Phys. Rev. 71, 413, 1947

14. G. E. Becker and Stanley H. Autler, Phys. Rev. 70, 300, 1946

15. J. R. Rusk, J. Chem. Phys. 42, 493, 15 January 1965

16. C. W. Tolbert, A. W. Straiton and J. H. Douglas, E. E. Res. LaC., Texas, Univ. of Texas No. 104, Nov. 1958

17. A. U. Straiton and C. W. Tolbert, Prac. IRE 48 page 898, 1960

18. G. T. Coats, R. A. Bond, C. W. Tolbert, E. E. Res. Lab., Univ of Texas Report No. 7-20, 1962

19. W. G. Benedict and L. D. Kaplan, J. Chem. Phys. 30, 388, 1959

20. See also: J. Quant Spectrosc. Radial Transfer 4, 453, 1963

21. J. C. Slater, Rev. Mod. Phys. 18, 180, 1946

22. G. Birnbaum, J. Chem. Phys. 27, 360, 1957

23. L. Frenkel, PhD Thesis, Univ of Maryland, 1964

24. G. W. King, R. M. Hainer and P. C. Cross, Phys. Rev. 71, 433, 1947

25. P. W. Anderson, Phys. Rev. 76, 647, 1949

26. J. O. Artman, Columbia Radiation Laboratory, Columbia Univ., June 1, 1953

27. J. H. Van Vleck, Phys. Rev. 71, 413, 1947

28. M. Tinkham and M. W. P. Strandberg, Phys. Rev. 97, 937, 1955

29. M. Mizushima, ASTIA Report, AD 242, 228

30. W. S. Benedict, Mem. Soc. Roy. Liege, Sp. Vol 2, 18, 1957

31. W. S. Benedict, H. H. Claassen and J. H. Shaw, J of Res. N.B.S. 49, 91, 1952

32. C. H. Townes, A. L. Schawlow, Microwave Spectroscopy, McGraw-Hill, 1955 (page 255)

33. G. R. Bird, J. Chem. Phys. 25, 1040, 1956

34. A. A. Maryott and G. Birnbaum, J. Chem. Phys. 36, 2026, 1962

35. R. Heastie and D. H. Martin, Canad J. of Phys. 40, 122, 1962

36. H. A. Gebbie and N. W. B. Stone, Proc. Phy. Soc. 82, 543, 1963.

APPENDIX A

LITERATURE SEARCH FOR ATMOSPHERIC ABSORPTION DATA

The status of work performed in the past on the absorption of electromagnetic radiation by atmospheric constituents was comprehensively reviewed as late as 1962 by Evans, Backynski and Wacker of RCA (AD294452), in 1961 by Schmelzer of Lockheed (AD256896), and in 1960 by W. T. Hunt of Wright Air Development Center (AD252126) and E. S. Rosenblum of MIT (AD242598). Each of these surveys contains an extensive reference list and a synopsis of the data available at that time. These references, as well as those appended to this report, reveal that most of the experimental work on the magnitude of microwave absorption by H_2O and O_2 in the atmosphere has been done by the University of Texas, Bell Telephone Laboratories and the Naval Research Laboratories.

Among the experimental data available from these sources, the highest frequency employed is 190 Gc by the University of Texas. This measurement, however, was not performed under rigorously controlled conditions. The data were obtained using a free space propagation range and a normal atmosphere, the characteristics of which could only be approximated. These data, therefore, are of limited value in the determination of line parameters of H_2O and O_2 and the prediction of higher frequency resonances.

The University of Texas does have superior instrumentation (500 foot absorption cell) for making measurements under controlled conditions and is currently instrumenting to obtain data in the region of the 183.3 Gc water vapor resonance line.

The most recent work on line breadth studies at 183.3 Gc was performed by J. R. Rusk of Aerospace Corporation. These constitute the most precise data available on self and foreign gas broadening of H_2O at 183.3 Gc, outside of the work performed on this contract.

As the literature also indicates, some work has been done on the location of molecular resonance frequencies of atmospheric constituents in the submillimeter and far infrared regions from both the theoretical and experimental points of view. The applicability of existing theory (References 1 and 41), however, depends heavily upon line parameters obtained through laboratory spectroscopic experimentation at lower frequencies.

Extensive data have been obtained on oxygen in the regions of 60 Gc and 120 Gc under various conditions. The contribution by oxygen at higher frequencies is negligible and, as a result, little or no data exist beyond 120 Gc.

The frequencies of the spectral lines of the earth's atmospheric constituents are listed by R. M. Vaillancourt (AD259918) for the range extending from 1 Gc to 250 Gc. Higher frequencies are tabulated by Schmelzer (AD256896) and McCubbin (Reference 8) extending into the far infrared.

Some work has been done to extend theory and measurements into the far infrared and submillimeter regions from the IR region using radiometric techniques and the equations of Van Vleck and Weisskopf. The works of Gebbie (Reference 13), Ryadov and Furashov (Reference 4), Yaroslavsky and Stanevich (Reference 9), and Zhevakin and Naumov (Reference 7), are typical of activity in this area.

Based on constants derived from measurements in the lower frequency regions, Zhevakin and Naumov (Reference 7) have calculated water vapor resonant frequencies and absorption coefficients for wavelengths extending from 10 microns to 2 centimeters (60 Gc to 30,000 Gc). Using long wavelength infrared spectroscopic techniques under laboratory atmospheric conditions, Yaroslavsky and Stanevich (Reference 9) confirmed the work of Zhevakin and Naumov in the 20 - 2500 micron region (120 Gc to 15,000 Gc). The data of Yaroslavsky and Stanevich indicate the presence of atmospheric windows near 0.35 mm (858 Gc) and in the region 1 mm to 1.5 mm (300 Gc to 200 Gc). Low attenuation is also shown at frequencies below the 183.3 Gc water vapor line (λ = 1.64 mm).

Using the methods of radio astronomy Ryadov and Furaskov (Reference 4) made detailed measurements of the transparency of the atmosphere at a wavelength of 0.87 millimeter. With some corrections, their data confirm those of Theissing and Caplan (Reference 14) in the range 0.9 to 3.6 mm.

In general, the work on atmospheric attenuation in the far infrared indicates a maximum in the region of 3000 Gc, with a gradual reduction in water vapor losses to about 0.5 db/kilometer at 30,000 Gc (Reference 7).

The bibliography has been compiled in two sections: Contract documents and reports available from ASTIA, and open literature. No attempt has been made to list all publications devoted to the absorption of electromagnetic energy. An attempt has been made to limit the bibliography to publications devoted to attenuation by atmospheric constituents above 30 Gc, i.e., the millimeter to far IR wavelength region.

Notes on significant aspects of some publications have been included.

REPORTS AVAILABLE FROM ASTIA

AD 98 763
Rotational Frequencies and Absorption Coefficients of Atmospheric Gases
S. N. Ghosh - March 1956
AF Cambridge Research Center

AD 283 989
Microwave Spectroscopy of Oxygen Molecule
Boulder, Colorado University
Masataka Mizushima - 31 August 1962

AD 259 918
Microwave Spectroscopic Data on the Earth's Atmosphere Constituents
R. M. Vaillancourt - April 1961
Canadian Armament Research and Development Establishment

AD 243 242
Survey of the Literature on Millimeter and Submillimeter Waves
Jerome Lurge, TRG Report - 129-SR-2
ARDC, Bedford, Mass.

AD 252 126
Survey of Attenuation by the Earth's Atmosphere at Millimeter Radio Wavelengths
Wade T. Hunt - November 1960
Reconnaissance Laboratory, Wright Air Development Division, Air Research and Development Command, USAFB, Wright-Patterson AFB, Ohio

AD 236 962
Research Studies in Connection with Microwave Spectrum of the O_2 Molecule
Masataka Mizushima - 1 January - 31 March 1960
Colorado University, Boulder

AD 242 228
Research Studies in Connection with Microwave Spectrum of the O_2 Molecule
Masataka Mizushima - 31 July 1960
Colorado University, Boulder

AD 243 352
Precise Measurement of the Microwave Absorption Frequencies of the Oxygen Molecule
Robert W. Zimmerer and Masataka Mizushima - September 1960
Colorado University, Boulder

AD 211 287
Research Studies in Connection with Microwave Spectrum of the O_2 Molecule

Masataka Mizushima - 1 October - 31 December 1958 20 January 1959
Colorado University, Boulder

AD 220 118
Research Studies in Connection with Microwave Spectrum of the O_2 Molecule
Masataka Mizushima - 1 April - 30 June 1959
Colorado University, Boulder

AD 233 525
Research Studies in Connection with Microwave Spectrum of the O_2 Molecule
Masataka Mizushima - 1 October - 31 December 1959
Colorado University, Boulder

AD 229 084
Research Studies in Connection with Microwave Spectrum of the O_2 Molecule
Masataka Mizushima, J. E. Drumheller and A. D. Sanchez - 1 July - 30 September 1959
Colorado University, Boulder

AD 257 843
Generation and Transmission of Electromagnetic Waves in the Terrestrial Atmosphere
P. J. Nawrocki and R. J. Papa - May 1961
Geophysics Corp. of America, Bedford, Mass.

AD 403 908
The Microwave Spectrum of Oxygen in the Earth's Atmosphere
M. L. Meeks - 25 October 1962
Lincoln Lab. MIT

AD 404 207
Design of Experiments for Remote Microwave Probing of the Atmosphere
B. R. Bean, R. L. Abbott and E. R. Westwater - 30 April 1963
National Bureau of Standards, Boulder, Colorado

AD 277 404
Transmission Loss in Radio Propagation: II
Kenneth A. Norton - June 1959
National Bureau of Standards, Washington, D.C.

AD 255 135
Curves of Atmospheric-Absorption Loss for Use in Radar Range Calculation
L. V. Blake - 23 March 1961
Naval Research Lab., Washington, D.C.

AD 51 293
Microwave Frequencies and Atmospheric Profiles
Dudley Williams
Ohio State University

AD 410 571
Absorption of Laser Radiation in the Atmosphere
Ronald K. Long - 31 May 1963
Ohio State University, Research Foundation, Columbus

AD 294 452
The Radio Spectrum from 10 Gc to 300 Gc in Aerospace Communications
Volume IV. Absorption in Planetary Atmospheres and Sources of Noise
A. Evans, M. P. Bachynski and A. G. Wacker - August 1962
RCA Victor Co., Ltd. (Canada)

AD 262 514
Research Activities in Millimeter Radiowaves and Geomagnetics
31 July 1961
Electrical Engineering Research Lab.,
University of Texas, Austin

AD 219 301
Propagation Studies Between 18.0 and 25.5 kmc/s
C. W. Tolbert, A. W. Straiton and C. O. Britt - 10 July 1959
Electrical Engineering Research Lab., University of Texas, Austin

AD 254 460
Calculated Values of Absorption Due to Water Vapor and Oxygen in the Millimeter Spectrum
C. W. Tolbert and R. M. Dickinson - 20 February 1961
Electrical Engineering Research Lab.,
University of Texas, Austin

AD 267 482
Research on Millimeter Wave Propagation at High Altitudes
30 November 1961
Electrical Engineering Research Lab.
University of Texas, Austin

AD 273 029
Research on Millimeter Wave Propagation at High Altitudes
28 February 1962
Electrical Engineering Research Lab.,
University of Texas, Austin

AD 407 421
Attenuation and Emission of 58 to 62 kmc/s Frequencies in the Earth's Atmosphere

31 March 1963
Electrical Engineering Research Lab.,
University of Texas, Austin

AD 414 410
Atmospheric Absorption of Electromagnetic Radiation in the Frequency Region 120 to 132 kmc/s Part II
C. O. Hemmi - 1963
Electrical Engineering Research Lab.,
University of Texas, Austin

AD 246 528
A Study and Analysis of Anomalous Atmospheric Water Vapor Absorption of Millimeter Wavelength Radiation
C. W. Tolbert - October 31, 1960
University of Texas

AD 414 361
A Spectroscopic Measurement of the Resonant Absorption of Microwave Energy by Oxygen in the 2.5-Millimeter Wavelength Region
A. E. Schulze - 1963
Electrical Engineering Research Lab.,
University of Texas, Austin

AD 285 111
Research on Millimeter Wave Propagation at High Altitudes
31 August 1962
Electrical Engineering Research Lab.,
University of Texas, Austin

AD 237 109
Radio Wave Absorption of Several Gases in the 100-117 kmc Frequency Range
C. O. Britt, C. W. Tolbert, and A. W. Straiton - 10 May 1960
Electrical Engineering Research Lab.,
University of Texas, Austin

AD 403 887
Research on Electromagnetic Wave Propagation Effects in Dynamic Situations
Electrical Engineering Research Lab.,
University of Texas, Austin

AD 227 989
The Spectral Band Between the Longwave Infrared and the Microwaves, Present Position and Tendencies of Development
M. Vogel - January 1959
Ministry of Supply, Great Britain

AD 256 896
Total Molecular Absorption in the Atmosphere for Frequencies Below 380 kmc
R. J. Schmelzer - March 1961
Lockheed Aircraft Corporation, Sunnyvale, California

AD 211 881
Research Investigation Directed Toward Extending the Useful Range of the Electromagnetic Spectrum
P. Kusch - 16 September - 15 December 1958
Columbia Radiation Lab, New York, N.Y.

AD 218 026
Research Investigation Directed Toward Extending the Useful Range of the Electromagnetic Spectrum
P. Kusch - 16 December 1958 - 15 March 1959
Columbia Radiation Lab., New York, N.Y.

AD 225 123
Research Investigation Directed Toward Extending the Useful Range of the Electromagnetic Spectrum
P. Kusch - 16 March - 15 June 1959
Columbia Radiation Lab., New York, N.Y.

AD 229 830
Research Investigation Directed Toward Extending the Useful Range of the Electromagnetic Spectrum
P. Kusch - 16 June - 15 September 1959
Columbia Radiation Lab., New York, N.Y.

AD 233 885
Research Investigation Directed Toward Extending the Useful Range of the Electromagnetic Spectrum
P. Kusch - 16 September - 15 December 1959
Columbia Radiation Lab., New York, N.Y.

AD 241 684
Research Investigation Directed Toward Extending the Useful Range of the Electromagnetic Spectrum
P. Kusch - 16 March - 15 June 1960
Columbia Radiation Lab., New York, N.Y.

AD 251 220
Research Investigation Directed Toward Extending the Useful Range of the Electromagnetic Spectrum
R. Novick - 16 September - 15 December 1960
Columbia Radiation Lab., New York, N.Y.

AD 256 477
Research Investigation Directed Toward Extending the Useful Range of the Electromagnetic Spectrum
R. Novick - 16 December 1960 - 15 March 1961
Columbia Radiation Lab., New York, N.Y.

AD 272 605
Research Investigation Directed Toward Extending the Useful Range of the Electromagnetic Spectrum
R. Novick - 15 December 1961
Columbia Radiation Lab., New York, N.Y.
Note: Absorption in Model Planetary Atmospheres

AD 275 422
Research Investigation Directed Toward Extending the Useful Range of the Electromagnetic Spectrum
R. Novick - 15 March 1962
Columbia Radiation Lab., New York, N.Y.

AD 400 457
Detection of the Microwave ν_{27}- Line of Molecular Oxygen Produced in the High Atmosphere
W. Kahan - 7 July 1962
Columbia Radiation Lab., New York, N.Y.

AD 405 530
Research Investigation Directed Toward Extending the Useful Range of the Electromagnetic Spectrum
R. Novick - 15 March 1963
Columbia Radiation Lab., New York, N.Y.

AD 415 961
(No Title)
Final Report - 1 May 1962 - 30 April 1963
Columbia University, New York, N.Y.

AD 418 059
Research Investigation Directed Toward Extending the Useful Range of the Electromagnetic Spectrum
R. Novick - 15 June 1963
Columbia Radiation Lab., New York, N.Y.

AD 418 446
Research Investigation Directed Toward Extending the Useful Range of the Electromagnetic Spectrum
R. Novick - 15 June 1963
Columbia Radiation Lab., New York, N.Y.

AD 414 123
Theory of Absorption Line Shapes in Monatomic Gases. I: General Formulation and Approximate Solutions
Hisao Takebe, Gene P. Reck and C. Alden Mead - 1962
Minnesota University School of Chemistry, Minneapolis, Minn.

AD 262 030
Research in Microwave Spectroscopy
John Sheridan - 31 December 1960
Birmingham University, (Great Britain)

AD 242 598
Atmospheric Absorption of 10-400 kmcps Radiation: Summary and Bibliography to 1960
E. S. Rosenblum - August 15, 1960
Massachusetts Institute of Technology, Cambridge, Mass.

REFERENCES TO APPENDIX A
(OPEN LITERATURE)

1. J. H. Van Vleck, "The Absorption of Microwaves by Uncondensed Water Vapor," Phys. Rev., 71, No. 7, April 1, 1947

2. G. W. King, R. M. Hainer, P. C. Cross; "Expected Microwave Absorption Coefficients," Phys. Rev., 71, No. 7, April 1, 1947

3. G. E. Becker, S. H. Autler; "Water Vapor Absorption of Electromagnetic Radiation in the Centimeter Wavelength Range," Phys. Rev., 70, Nos. 5 and 6, September 1 and 15, 1946

4. V. Y. Ryadov, N. I. Furashov, and G. A. Sharonov; "Measurement of Atmospheric Transparency to 0.87 mm Waves," Radio Engineering and Electronic Physics, Vol. 9, June 1964

   Notes: Sun observations at λ = 0.87 mm (345 Gc) "window" provided a measured loss of 8.5 db/km for P = 7.5 g/m^3 and P = 760 mm Hg.

5. T. F. Rogers; "Absolute Intensity of Water Vapor Absorption at Microwave Frequencies," Phys. Rev., 26 October 1953

   Notes: Confirms VV-W modified Lorentz equation for collision broadening out to frequencies removed several linewidths from resonance at 1 cm (30 Gc).

6. N. Ginsburg; "Additional Rotational Energy Levels of H_2O and D_2O Molecules," Phys. Rev., 47, No. 9, November 1, 1948

7. S. A. Zhevakin, A. P. Naumov; "Coefficient of Absorption of Electromagnetic Waves by Water Vapor in the Range 10μ to 2 cm; Russian translation, (Izvestia Vuzov NVSSO, SSSR, Radio FIZIKA, 1963, 6, 4, 674)

   Notes: Cites calculations using dynamic equations from 60 Gc to 30,000 Gc emphasizing reduction of losses around 30,000 Gc. Cites good agreement w/russian data above 500 Gc.

8. McCubbin, T. King, Jr.; "The Spectra of HC1, NH_3, H_2O, and H_2S from 100 to 700 Microns," The Journal of Chemical Physics, 20, No. 4, April 1952

   Notes: 428 Gc to 3000 Gc.

9. N. G. Yaroslavsky, A. E. Stanevich; "The Long Wavelength Infrared Spectrum of H_2O Vapor and the Absorption Spectrum of Atmospheric Air in the Region 20 - 2500μ (500 - 4 cm^{-1}), (Optika i Spektroskopiya - Optics and Spectroscopy - 7, 621 (1959) Russian translation. Incoherent sources and detectors.

10. W. S. Benedict, E. K. Plyler; "Absorption Spectra of Water Vapor and Carbon Dioxide in the Region of 2.7 Microns," Journal of Research of the National Bureau of Standards, Vol. 46, No. 3, March 1951

11. Alvin Meckler; "Electronic Energy Levels of Molecular Oxygen," The Journal of Chemical Physics, Vol. 21, No. 10, October 1953

12. R. S. Anderson, C. M. Johnson, Walter Gordy; "Resonant Absorption of Oxygen at 2.5- Millimeter Wavelength," Physical Review, Letters to the Editor, July 16, 1951

13. H. A. Gebbie, et al; Physical Review, 107, 1194 (1957, J. Phys. Radium, 19, 230 (1958) Nature, 178, 432 (1958, Prac. Roy. Sac., A-206, 87 (1951) Nature, 187, 765 (1960)

14. H. H. Theissing, and P. J. Caplan; "Atmospheric Attenuation of Solar Millimeter Wave Radiation," Journal of Applied Physics, 27, 5, 538 (1956)

15. George Birnbaum; "Millimeter Wavelength Dispersion of Water Vapor," Journal of Chemical Physics, 21, 1, (1953)

16. C. Greenhow and William V. Smith; "Molecular Quadrupole Moments of N_2 and O_2," Journal of Chemical Physics, 19, 10, (1951)

17. M. L. Meeks; "Atmospheric Emission and Opacity at Millimeter Wavelengths Due to Oxygen," Journal of Geophysical Research Vol. 66, No. 11 1961, November

18. W. R. Bandeen, R. A. Hanel, John Licht, R. A. Stampfl, and W. G. Stroud; "Infrared and Reflected Solar Radiation Measurements from the Tiros II Meteorological Satellite," Journal of Geophysical Research Vol. 66, No. 10 October 1961

19. James H. Burkhalter, Roy S. Anderson, William V. Smith, and Walter Gordy; "A Preliminary Report on the Fine Structure of the Microwave Absorption Spectrum of Oxygen," Department of Physics, Duke University, Physical Review - Letters to Editor, November 23, 1949

20. A. A. Maryott, G. Birnbaum; "Microwave Absorption in Compressed Oxygen," Physical Review, Vol. 99, No. 6, September 15, 1955 Letters to the Editor

21. B. V. Gokhale, and M. W. P. Strandberg; "Line Breadths in the 5-mm Microwave Absorption of Oxygen," Physical Review, 84, 844 (1951)

22. Robert Beringer; "Absorption in Oxygen at One-Half cm," Radiation Laboratory, Massachusetts Institute of Technology. American Phys. Soc. Mtg.

23. R. L. Kyhl, R. H. Dicke, and Robert Beringer; "The Absorption of 1-cm Electromagnetic Waves by Atmospheric Water Vapor," Radiation Laboratory, Massachusetts Institute of Technology. American Phys. Society Mtg.

24. B. V. Gokhale, and M. W. P. Strandberg; "Microwave Absorption Spectrum of Oxygen," Massachusetts Institute of Technology, American Physical Society Meeting

25. M. Tinkham, and M. W. P. Strandberg; "Selection Rules in the Microwave Magnetic Resonance Spectrum of Oxygen," Massachusetts Institute of Technology, American Physical Society Meeting

26. Charles A. Burrust, and Walter Gordy; "Submillimeter Wave Spectroscopy," Physical Review, Page 897, February 1954

27. C. H. Townes, and F. R. Merritt; "Water Spectrum Near One-Centimeter Wavelength," Bell Telephone Laboratories

28. Roy S. Anderson, William V. Smith, and Walter Gordy; "Line Breadths of the Fine Structure of the Microwave Spectrum of Oxygen," Physical Review, P. 264, April 1951

29. M. W. P. Strandberg, C. Y. Meng, and J. G. Ingersoll; "The Microwave Absorption Spectrum of Oxygen," Physical Review, Vol. 75, No. 10, May 15, 1949

30. Roy S. Anderson, William V. Smith, Walter Gordy; "Line Breadths of the Microwave Spectrum of Oxygen," Physical Review, Vol. 87, No. 4, August 15, 1952

31. A. Abragam, and J. H. Van Vleck; "Theory of the Microwave Zeeman Effect in Atomic Oxygen," Physical Review,Vol. 92, No. 6, December 1953

32. Robert H. Dicke, Robert Beringer, Robert L. Kyhl, and A. B. Vane; "Atmospheric Absorption Measurements with a Microwave Radiometer," Physical Review, Vol. 70, No. 5 and 6, September 1 and 15, 1946

33. James H. Burkhalter, Roy S. Anderson, William V. Smith, and Walter Gordy; "The Fine Structure of the Microwave Absorption Spectrum of Oxygen," Physical Review, Volume 79, No. 4, August 15, 1950

34. Henry Margenau; "Statistical Theory of Pressure Broadening," Physical Review, Vol. 82, No. 2, April 15, 1951

35. J. O. Artman, and J. P. Gordon; "Absorption of Microwaves by Oxygen in the Millimeter Wavelength Region," Physical Review, Vol. 96, No. 5 December 1, 1954

36. S. L. Miller, C. H. Townes, and M. Kotani; "The Electronic Structure of O_2," Physical Review, Vol. 90, No. 4, May 15, 1953

37. D. W. Posener, and M. W. P. Strandberg; "Centrifugal Distortion in Asymmetric Top Molecules. III. H_2O, D_2O, and HDO," Physical Review, Vol. 95, No. 2, July 15, 1954

38. Masataka Mizushima, and Robert M. Hill; "Microwave Spectrum of O_2," Physical Review, Vol. 93, No. 4, February 15, 1954

39. William C. King, and Walter Gordy; "One-To-Two Millimeter Wave Spectroscopy. IV. Experimental Methods and Results for OCS, CH_3F, and H_2O," Physical Review, Vol. 93, No. 3, February 1, 1954

40. Robert Beringer; "The Absorption of One-Half Centimeter Electromagnetic Waves in Oxygen," Physical Review, Vol. 70, Nos. 1 and 2 July 1 and 15, 1946

41. J. H. Van Vleck; "The Absorption of Microwaves by Oxygen," Physical Review, Vol. 71, No. 7, April 1, 1947

42. Robert M. Hill, and Walter Gordy; "Zeeman Effect and Linebreadth Studies of The Microwave Lines of Oxygen," Physical Review, Vol. 93 No. 5, March 1, 1954

43. M. Tinkham, and M. W. P. Strandberg; "Theory of the Fine Structure of the Molecular Oxygen Ground State," Physical Review, Vol. 97, No. 4, February 15, 1955

44. S. L. Miller, and C. H. Townes; "The Microwave Absorption Spectrum of $(O^{16})_2$ and $O^{16}O^{17}$," Physical Review, Vol. 90, No. 4, May 15, 1953

45. M. Lichtenstein, J. J. Gallagher, and R. E. Cupp; "Millimeter Spectrometer Using a Fabry-Perot Interferometer," Review of Scientific Instruments, Vol. 34, No. 8, 843-846, August 1963

46. Victor K. Chung; "Absorption and Emission of Atmospheric Water Vapor," Massachusetts Institute of Technology Report No. N64-10915

47. M. L. Meeks; "Oxygen Emission and Absorption," Massachusetts Institute of Technology Report No. N64-10912

48. A. Battaglia, A. Gazzini, and M. Lannuzzi; "Millimeter Wave Absorption, Oxygen," Arch. Sci. (Switzerland) Vol. 14, Spec. No. 93-101 (September 1961)

49. S. Chandra, and B. P. Srivastava; "Absorption of Microwaves in Planetary Atmospheres," Zeitsckrift fur Astrophysik, Vol. 47, No. 2, PP-127-134 (1959)

50. T. F. Rogers; "Microwave and Far Infrared Atmospheric Water Vapor Absorption, "Air Force Cambridge Research Center

51. P. W. Anderson; "On the Limits of Validity of the Van Vleck - Weisskopf Line Shape Formula," Bell Telephone Laboratories

52. J. E. Walter, and W. D. Hershberger; "Absorption of Microwaves by Gases II," RCA Laboratories, Princeton, New Jersey

APPENDIX B

COMPILATION OF ATMOSPHERIC ABSORPTION DATA AND EXTRAPOLATION TO 1000 Gc

The references cited in Appendix A contain numerous compilations, experimental as well as theoretical, of atmospheric absorption data as functions of altitude and frequency.

The most complete data consistent with the parameters measured in this work are those of Schmelzer (AD 256896) and these are included for convenience with this report. (Tables VII, VIII, and IX.)

Extrapolations to 1000 Gc have been made by Zhevakin and Naumov*. These have been amended in the light of data reported here, and are shown in Figure 19.

* "Coefficient of Absorption of Electromagnetic Waves by Water Vapor in the Range 10μ to 2 cm;" Russian translation, (Izvestia Vuzov NVSSO, SSSR, Radio FIZIKA, 1963, 6, 4, 674)

TABLE VII

Atmospheric Absorption, Oxygen

Altitude h (km)	Attenuation Coefficient (db/km) at Indicated Frequencies (mc) 60,435	60,439	60,440	60,465
0	16.14	16.122	16.118	16.00
5	13.64	13.60	13.58	13.30
10	12.20	12.14	12.12	11.64
15	9.94	9.90	9.88	8.78
20	9.12	9.02	8.96	5.64
25	8.90	8.44	8.22	2.22
30	8.02	6.26	5.56	0.478
35	7.24	3.12	2.36	0.0972
40	6.44	0.995	0.674	0.0212
50	4.94	0.078	0.0498	0.00142
60	–	0.0128	0.0082	–
70	3.74	0.002	0.0014	–
80	1.48	0.0004	–	–
90	0.266	0.00006	–	–
100	0.040	0.00001	–	–

Source: AD 256 896, page 2-7 Schmelzer, Lockheed 1961

TABLE VIII

Water Vapor Attenuation

Altitude h (km)	Attenuation (db/km) at Indicated Frequencies ν (kmc)						
	18.0	22.25	30.0	37.5	60.0	184.4	210.0
0	0.0418	0.159	0.0643	0.0613	0.125	27.9	2.27
1	0.0278	0.121	0.0417	0.0397	0.0816	22.1	1.48
2	0.0169	0.0842	0.0248	0.0237	0.0491	16.1	0.894
3	0.0103	0.0600	0.0149	0.0142	0.0296	12.0	0.541
4	0.0055	0.0371	0.0078	0.0075	0.0157	7.77	0.287
5	0.0031	0.0248	0.0043	0.0042	0.0088	5.43	0.162
6	0.0015	0.0146	0.0021	0.0021	0.0044	3.35	0.081
7	0.0008	0.0092	0.0011	0.0011	0.0023	2.23	0.043
8	0.0004	0.0051	0.0005	0.0005	0.0011	1.29	0.020
9	0.0002	0.0030	0.0002	0.0002	0.0005	0.815	0.010
10	0.0001	0.0015	0.0001	0.0001	0.0002	0.441	0.004
11	0.0000	0.0009	0.0000	0.0000	0.0001	0.258	0.002
12	0.0000	0.0006	0.0000	0.0000	0.0005	0.180	0.001
Total db	0.0874	0.441	0.130	0.124	0.256	85.7	4.66

Altitude h (km)	Attenuation (db/km) at Indicated Frequencies ν (kmc)						
	222.3	270.0	324.0	333.0	341.0	354.0	380.0
0	2.33	4.25	37.81	13.32	12.05	13.9	289
1	1.52	2.78	28.44	8.97	7.93	9.11	227
2	0.917	1.67	19.75	5.63	4.81	5.49	164
3	0.556	1.014	14.06	3.44	2.93	3.32	121
4	0.295	0.541	9.73	2.05	1.61	1.78	77.6
5	0.167	0.303	5.84	1.113	0.881	0.993	53.7
6	0.083	0.152	3.46	0.567	0.441	0.496	32.8
7	0.044	0.080	2.21	0.305	0.233	0.261	21.5
8	0.020	0.037	1.226	0.143	0.108	0.121	12.3
9	0.010	0.018	0.745	0.071	0.053	0.060	7.69
10	0.004	0.008	0.396	0.030	0.023	0.025	4.10
11	0.002	0.004	0.223	0.014	0.010	0.012	2.38
12	0.001	0.002	0.019	0.004	0.005	0.006	1.67
Total db	4.79	8.74	104.6	28.8	25.0	28.6	869.

Source: AD 256 896, Page 3-12 Schmelzer, Lockheed 1961

TABLE IX

Total Atmospheric Absorption (db/km)

Range of Altitude h (km)	Absorption at Indicated Frequencies ν (mc)			
	60,435	60,439	60,440	60,465
0 to 100	585	578	575	504
10 to 100	447	220	209	114
15 to 100	392	166	155	63
20 to 100	345	119	108	26.5
25 to 100	299	75.7	65	7.4
30 to 100	257	35.3	29.1	1.57
35 to 100	219	14.7	10.6	0.387
40 to 100	185			

Source: AD 256 896, Page 2-11, Schmelzer, Lockheed, 1961

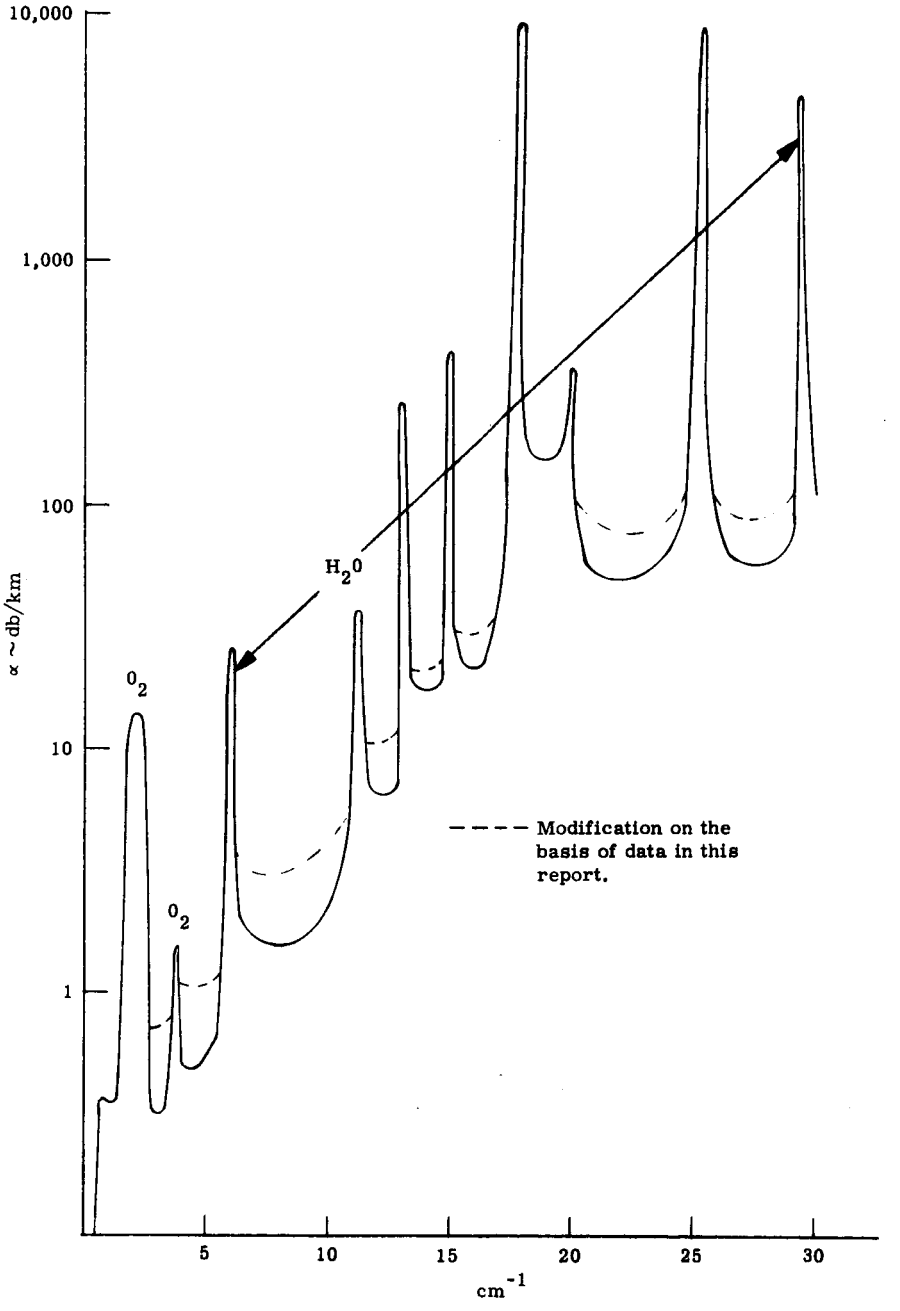

Figure 19. Approximate Peaks and Windows in Atmospheric Attenuation, p = 760 mm Hg, 50 Percent Humidity (After Zhevakin and Naumov)

APPENDIX C

CONTRACT NASw-963
STATEMENT OF WORK

Phase I

Perform an analysis and comparison of the Q predicted for the Fabry-Perot interferometers to be developed with that necessary to make useful measurements.

Phase II

Measure the absorption of oxygen and water vapor in the presence of gases such as nitrogen, carbon dioxide and ammonia.

Task 1

Search for rotational transitions of oxygen at 368, 424, and 487 gigacycles and measure the linewidths as a function of pressure and temperature.

Task 2

Study interferometer measurement techniques and associated components for which development is needed.

Task 3

Measure the absorption due to water vapor in the windows near 140, 250, 340 and 400 gigacycles.

Task 4

Compile and plot data of absorption below 500 gigacycles as a function of altitude and extrapolate this data to project what might be expected at frequencies up to 1,000 gigacycles.